Geochemistry Geophysics Geosystems G3

Article
Volume 12, Number 10
21 October 2011
Q10015, doi:10.1029/2011GC003706
ISSN: 1525-2027

Published by AGU and the Geochemical Society

Measurements and uncertainties of the occurrence time of the 1969, 1978, 1991, and 1999 geomagnetic jerks

K. J. Pinheiro
Observatorio Nacional, General Jose Cristino, 77, Sao Cristovao, CEP: 20921-400, Rio de Janeiro, Brazil (kpinheiro@on.br)

A. Jackson and C. C. Finlay
Institut für Geophysik, ETH Zurich, Sonneggstrasse 5, CH-8092 Zurich, Switzerland

[1] Geomagnetic jerks are rapid time variations of the magnetic field at the Earth's surface that are thought to be of primarily internal origin. Jerks are relevant for studies of the Earth interior: they likely give information on core dynamics and possibly on mantle electrical conductivity. In such studies a precise determination of the jerk occurrence time and its error bar at each observatory is required. We analyze the most well-known global jerks (1969, 1978, and 1991) and a possible local jerk in 1999, considering all three components of the magnetic field (*X*, *Y*, and *Z*). Different data sets are investigated: annual means, 12 month running averages of observatory monthly means in rotated geomagnetic dipole coordinates, and data representing the core field contribution synthesized from the CM4 time-dependent field model. The secular variation in each component of the field around the time of a jerk was modeled by two straight line segments, using both least squares and 1-norm methods. The 1969, 1978, and 1991 jerks were globally detected, while the 1999 event was only locally identified. Using this simple method enables us to calculate error bars in the jerk occurrence times and to quantify their nonsimultaneous behavior. We find that our error bars are not, in general, symmetric about the mean occurrence time and that the mean errors on the *X* and *Z* components of 1.7 years and 1.5 years are larger than that of 1.1 years on the *Y* component. Generally, the error bars were found to be larger in the Southern Hemisphere observatories. Our results are necessary prerequisites for further studies of the inverse problem that attempt to determine mantle electrical conductivity from variations in jerk occurrence times.

Components: 12,400 words, 14 figures, 6 tables.

Keywords: data analysis; geomagnetic jerks; secular variation.

Index Terms: 1530 Geomagnetism and Paleomagnetism: Rapid time variations; 1560 Geomagnetism and Paleomagnetism: Time variations: secular and longer.

Received 16 May 2011; **Revised** 22 July 2011; **Accepted** 23 July 2011; **Published** 21 October 2011.

Pinheiro, K. J., A. Jackson, and C. C. Finlay (2011), Measurements and uncertainties of the occurrence time of the 1969, 1978, 1991, and 1999 geomagnetic jerks, *Geochem. Geophys. Geosyst.*, *12*, Q10015, doi:10.1029/2011GC003706.

1. Introduction

[2] The main magnetic field, generated in the core, varies in time and space. The complex variation in time exhibits behavior on many time scales, from minutes to millennia. On the time scale of years to decades is one of the most enigmatic of phenomena, termed geomagnetic jerks. We refer to the first

time derivative of the magnetic field as the secular variation (SV). Geomagnetic jerks are abrupt variations in the secular variation that typically have a "V" shape. The difference of slope of these secular variations is called the jerk amplitude. Amongst the most debated aspects of geomagnetic jerks are their morphologies (the spatial distribution of amplitude), the allied question of local or global visibility, and whether the same jerk is observed simultaneously or not at the Earth's surface. The nonsimultaneity of jerks has been used in attempts to obtain some information about mantle electrical conductivity [e.g., *Mandea Alexandrescu et al.*, 1999; *Nagao et al.*, 2003; *Pinheiro and Jackson*, 2008]. These studies depend critically on accurate measurements of the time when jerks are seen at magnetic observatories. We refer to this time as the occurrence time of a jerk.

[3] Many methods to detect the time when the jerk occurs at the surface have been explored in the past 30 years, the most common being the fitting of two straight line segments to the SV by a least squares method. This method is purely empirical and is not based on any theoretical model; it does however, serve as a good method to determine occurrence time. *Le Mouël et al.* [1982] analyzed more than 130 observatories by fitting straight lines to the SV before and after 1970. They assume that this jerk occurs at the same time at all observatories. Later, *Gubbins and Tomlinson* [1986] found that the 1970 jerk was not simultaneous at the Earth surface by finding a time lag of about 2 years between Apia (Samoa) and Amberley (New Zealand) observatories. *Whaler* [1987] also investigated the nonsimultaneity of jerks by fitting many possible straight line segments to the SV and measuring the optimal time for the change in slope.

[4] Wavelet analysis is another method widely used for the analysis of geomagnetic jerks; it was first globally applied by *Alexandrescu et al.* [1996]. This method involves the assumption that sudden events of an unknown nature at undefined dates may have occurred in the geomagnetic field. The sensitivity of wavelets to local characteristics of a signal is an important advantage of this method [*Alexandrescu et al.*, 1995]. *Alexandrescu et al.* [1996] considered a linear combination of X and Y components of observatory monthly means and detected seven different events: the 1901, 1913 and 1925 jerks were possibly global in extent but the 1932 and 1949 jerks were observed only in the Pacific and American areas, whereas the 1969 and 1978 jerks were found to be worldwide.

[5] *De Michelis and Tozzi* [2005] also applied wavelet analysis to detect jerks, by using 44 observatories (only 6 being in the Southern Hemisphere) and detected global jerks in 1978, 1991 and 1999 and a local jerk in 1986. One limitation of wavelet analysis is that the boundary effects are important, preventing detection of events close to the beginning and end of the time series. If the jerk is near one of the data limits it is necessary to apply more classical methods, as was carried out by *Mandea et al.* [2000] for the 1999 event.

[6] Jerks are also characterized by their amplitudes and most of the studies use spherical harmonic models. One example is *Le Huy et al.* [1998] who performed a spherical harmonic analysis of the 1969, 1978 and 1991 jerks. One of the problems of global models is the poor geographical distribution of observatories. This limitation can be overcome by the use of satellite data. *Sabaka et al.* [2004] developed a comprehensive model (CM4) over the time interval from 1960 to mid-2002, using observatory and satellite data. They were able to detect the well known jerks and discussed the possibility of an additional event around 1997.

[7] *Chambodut and Mandea* [2005] used the CM4 comprehensive model to separate internal from external sources and confirmed the nonsimultaneous behavior of the 1969, 1978 and 1991 jerks. However, *Olsen and Mandea* [2007] found a new jerk at 2003, by using satellite data, which is simultaneous at the Earth surface and has a local characteristic: it is only observed in a restricted area near 90°E and ±30° latitude. *Olsen and Mandea* [2008] inferred the existence of another localized jerk at 2005 centered on Southern Africa and *Chulliat et al.* [2010] reported a jerk in 2007 intense in the South Atlantic Region, that is anticorrelated with the 2003 jerk.

[8] There is a confusion over the precise definition, even phenomenological, of a jerk [*Mandea and Olsen*, 2009]. Thus, even nonglobal events are referred to as jerks, and two jerks which are only two years apart [*Olsen and Mandea*, 2008] continue to be referred to as jerks, though the independence of such events is questionable. What is lacking in all previous studies is the provision of error bars (uncertainty estimates) on the defining quantities. We provide these uncertainties for the first time in this paper. In this study we also restrict ourselves to study jerks that are relatively well spaced in time.

[9] The internal origin of geomagnetic jerks was demonstrated by *Malin and Hodder* [1982] using

spherical harmonic analysis. In a different approach, *Nagao et al.* [2002] applied a statistical time series model to geomagnetic monthly means data, adjusting seasonal and short time scale variations. They tested the possibility of the ring current as the origin of jerks and concluded that jerks cannot be explained by changes in latitudinally dependent external current, excluding the magnetospheric ring current as a source for jerks. However, *Alldredge* [1977] and *Alldredge* [1984] showed how external effects may introduce the typical "V" shape in the secular variation and influence jerk detection. Whether the detection of jerks is affected by external fields will depend on the data and methodology used to exclude most of the external signal and obtain a better defined jerk internal signal.

[10] Whether jerks are local or global, and simultaneous or not, depend on how they are generated in the core and how the electrically conducting mantle changes the original signal. One might imagine a jerk as the result of a rapid variation originating at the core surface, that is simultaneous everywhere. *Pinheiro and Jackson* [2008] considered this scenario and showed that mantle conductivity can lead to different occurrence times over the Earth's surface. Such an idealization gives the chance to glean some properties of the mantle's electrical conductivity distribution. An alternative model might invoke negligible effects of the mantle conductivity and a much more complex model of the core origin, involving nonsimultaneity. Either way, reliable uncertainty estimates on the jerk morphology are required.

[11] The plan for the paper is as follows: in section 2 we describe the three data sets used in this work: annual means, 12 month running average and the core field calculated by CM4 model. The methodology of fitting two straight lines to the secular variation is applied in section 3. Contrary to previous studies this enables us to calculate error bars on jerk occurrence times and to quantitatively determine those observatories where occurrences are either early or late. Results for the 1969, 1978, 1991 and 1999 jerks are presented in section 4 and comparisons to previous work discussed in section 5.

2. Data

[12] We analyzed three different data sets in order to study geomagnetic jerks in the X, Y and Z components of the geomagnetic field: observatory annual means; 12 month running averages of observatory monthly means in rotated geomagnetic dipole coordinates and annual means of the core field contribution calculated from the CM4 field model. Jerks were first studied using annual means but rapid events such as the 2003, 2005 and 2007 jerks have recently been studied using the higher temporal resolution provided by the secular variation estimates calculated from monthly means. The advantage of using a comprehensive model (CM4) is that such a model has attempted to separate different magnetic field sources: core, crustal, ionospheric, magnetospheric, induced and toroidal field produced by electrical currents at satellite altitudes [*Sabaka et al.*, 2002].

[13] In this paper, the secular variation is evaluated as the annual differences of main field data (e.g. $\frac{dY}{dt}|_{t_0} = Y(t_0 + \frac{1}{2}) - Y(t_0 - \frac{1}{2})$), with t_0 in years. Examples of observatory annual mean secular variation together with the CM4 prediction of the core field and monthly mean secular variation rotated to geomagnetic dipole coordinates are shown for the X, Y and Z components of Niemegk observatory (Germany) in Figures 1a–1f. Notice that using a 12 month running average of first differences of observatory monthly means gives the advantage of a higher temporal resolution, but these data also present a considerable amount of scatter that makes the identification of jerks more difficult than in the first difference of annual means. Furthermore, comparing the X, Y and Z components (Figures 1a–1f) it is clear that jerks are not simultaneous in the three components and that they are often more visible in the Y component, since it is less contaminated by external field variations.

[14] Annual mean data are provided by the World Data Centre (WDC) for Geomagnetism at the British Geological Survey (BGS, Edinburgh), while monthly means were obtained by the World Monthly Means Database Projects reported by *Chulliat and Telali* [2007]. The latter were derived from WDC hourly means with three consistency tests performed: visual inspection, comparison of monthly means with annual means, and comparison with results of the CM4 model. We excluded the months in which the mean was calculated from less than 15 days of data.

[15] In order to decrease the influence of magnetospheric fields on the X and Y components, monthly means data were rotated in geomagnetic dipole coordinate, by aligning the Northward and Eastward components with the geomagnetic dipole axis and also perpendicular to it [e.g., *Olsen and Mandea*, 2007]. For example, the dipole field direction for the

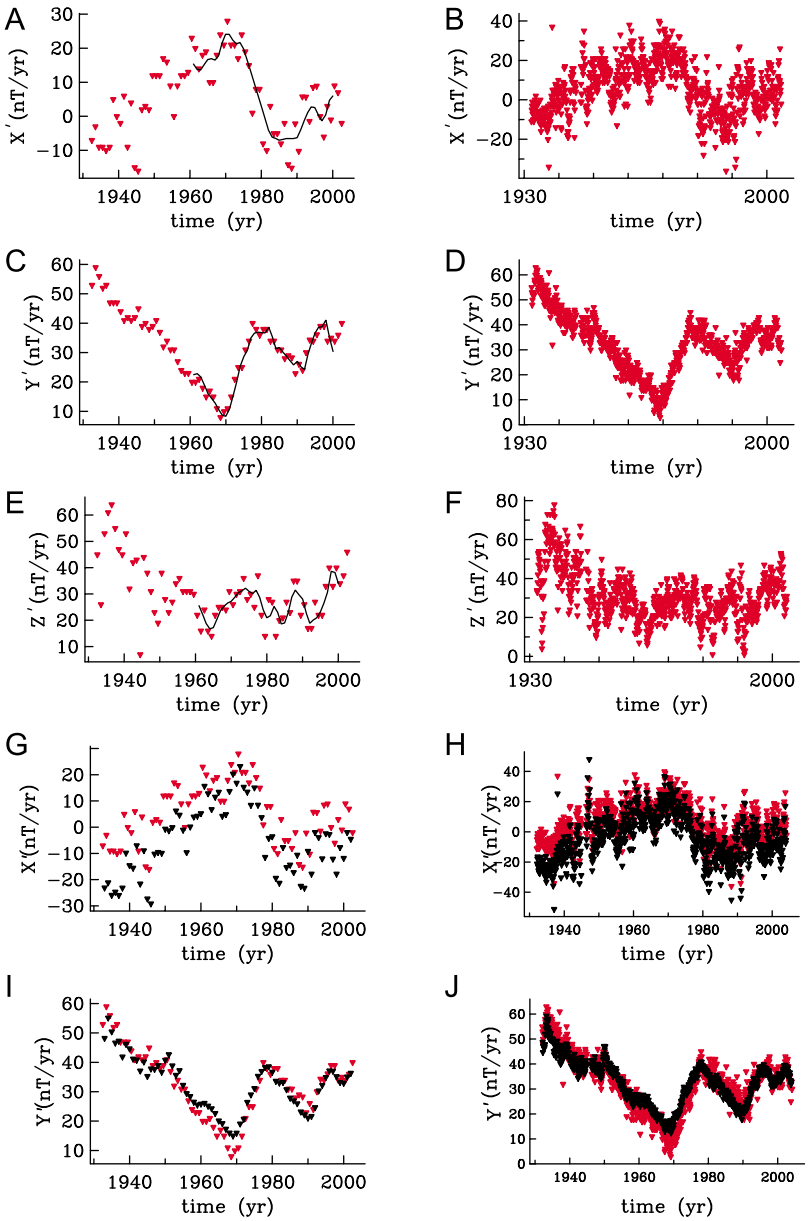

Figure 1. Secular variation estimates for the *X*, *Y*, and *Z* components of the magnetic field using different data sets at Niemegk observatory (Germany). (a, c, e) First differences of annual means (red triangles) and the core contribution secular variation evaluated by the CM4 model (black line) of the *X*, *Y*, and *Z* components, respectively. (b, d, f) The 12 month running averages of the first differences of monthly means in geographical coordinates (red triangles are shown). (g and i) The annual differences in geographical (red triangles) and geomagnetic dipole (black triangles) coordinates for the *X* and *Y* components, respectively. (h and j) The first differences of 12 month running average of monthly means for the *X* and *Y* components, respectively.

1969 jerk is taken to be the International Geomagnetic Reference Field (IGRF-10) definitive model for 1970 and the position of the dipole axis is given by a colatitude θ_{dip} = 11.41° and longitude ϕ_{dip} = 289.82°E. In some observatories such as Niemengk (Germany) this rotation of coordinates substantially decreases the amount of scatter present in the data (Figures 1g–1j) since the angle between the geographic and dipole coordinates is 18°, while at others such as Gnangara (Australia) this angle is about 2°, consequently the result does not differ greatly from the original data. We do not apply this rotation to annual means since in many cases we find it does not greatly reduce the noise.

[16] The analysis of each geomagnetic jerk is carried out separately: a complete set of data is considered to be 15 years of data, with 7 years before and 7 years after the supposed jerk. Most European observatories have complete annual mean data sets available for the 1969–1970 jerk, that is data from 1962 to 1976. However, we also include observatories with incomplete data sets, by which we mean a minimum of 11 years of data of which 5 years are centered at the date of the jerk (from 1968 to 1972 for the 1969–1970 jerk).

3. Methodology

3.1. Jerk Time and Amplitude Detection

[17] Geomagnetic jerks are modeled here as two straight line segments fit to the secular variation estimates. Denoting with C an arbitrary geomagnetic component, our parametric model is defined as

$$\dot{C}(t) = a_1(t - t_0) + b, \qquad \text{for } t \le t_0 \tag{1}$$

and

$$\dot{C}(t) = a_2(t - t_0) + b, \qquad \text{for } t \ge t_0 \tag{2}$$

In this model the intersection of the two straight lines defines the jerk occurrence time (t_0) and the jerk amplitude is given by

$$\mathcal{A} = a_2 - a_1, \tag{3}$$

for a given t_0. The three parameters (a_1, a_2 and b) define a model vector $\mathbf{m}$. The advantage of using this simple model is that we are able to calculate the required error bars on the occurrence time t_0 and the amplitude of geomagnetic jerks.

[18] In order to find the model that best fits the data, we explore different norms indicated by $||\mathbf{e}||$, the norm of the error (or residual) vector $\mathbf{e}$, where

$$\mathbf{e} = \mathbf{d} - \mathbf{G}(t_0)\mathbf{m}, \tag{4}$$

where $\mathbf{d}$ and $\mathbf{m}$ are the data and model vectors respectively, and $\mathbf{G}(t_0)$ relates $\mathbf{m}$ to the observations. We calculated the model parameters ($\mathbf{m} = \{a_1, a_2, b\}$) for all t_0 at intervals of 0.001 yr.

[19] We used L_1 and L_2 norms, $||\mathbf{e}||_1 = \sum_i |e_i|$ and $||\mathbf{e}||_2 = \sum_i |e_i|^2$, respectively. The choice of a norm implies an assumption that data errors obey a particular type of statistics: the L_2 norm (or least squares method) assumes a Gaussian distribution of errors while the L_1 norm assumes a Laplacian distribution. Long-tailed distributions, such as the Laplacian, imply many large residuals while short-tailed distributions, such as the Gaussian, tolerate less the presence of large outliers [e.g., *Menke*, 1989]. In geomagnetism the least squares method is usually used, in which data errors are assumed to be Gaussian. However, situations in which the distribution of the errors is known a priori are rare in geophysical problems and the assumption of Gaussian errors in geomagnetism is often motivated on grounds of simplicity. *Walker and Jackson* [2000] showed that in certain geomagnetic contexts a Laplacian error distribution maybe more appropriate than the Gaussian. For this reason, both L_1 and L_2 measures of data fit are considered in this work.

[20] The preferred value for t_0, for each geomagnetic jerk at each observatory and for each field component, is chosen from the minimum of the misfit curve and the error bars determined by intervals of confidence on the associated probability distribution function (PDF) curve. When the PDF is broad, there are many possible models in the neighborhood of the minimum misfit value that can fit the data to a satisfactory level; in this case the error bars are large. Conversely, when the PDF curve is sharp, the error bars become smaller since the minimum value of the misfit is well defined.

[21] In the case of a Gaussian distribution of errors, the probability of the data $\mathbf{d}$ given their predicted value $\mathbf{G}$ (t_0) $\mathbf{m}$ and their error bars α is

$$prob(\mathbf{d}|\mathbf{m}, \alpha, t_0, L_2) = \frac{1}{\alpha\sqrt{2\pi}} \exp\left[-\frac{(\mathbf{d} - \mathbf{G}(t_0)\mathbf{m})^T(\mathbf{d} - \mathbf{G}(t_0)\mathbf{m})}{2\alpha^2}\right], \tag{5}$$

but the problem in the present scenario is that the data error bars (α) are unknown [*Menke*, 1989]. An estimate of α, called $\hat{\alpha}$, can be inferred from the data, as shown by *Sivia and Skilling* [2006, chapter 3]:

$$\hat{\alpha} = \sqrt{\frac{\chi^2_m}{N - Tr(\mathbf{R})}}, \tag{6}$$

where χ^2_m is the minimum value of χ^2 at the optimal t_0, N is the number of independent data whose noise is assumed uncorrelated, $Tr(\mathbf{R})$ is the trace of the resolution matrix ($\mathbf{R} = [\mathbf{G}^T\mathbf{G}]^{-1}\mathbf{G}^T\mathbf{G}$) and considering the 3 parameters in our model, $Tr(\mathbf{R}) = 3$. χ^2 is defined as the sum of the squares of the residuals:

$$\chi^2 = \sum_i \left(d_i - \sum_j G_{ij}m_j\right)^2 = \sum_i e_i^2 = \| \mathbf{e} \|_2 \tag{7}$$

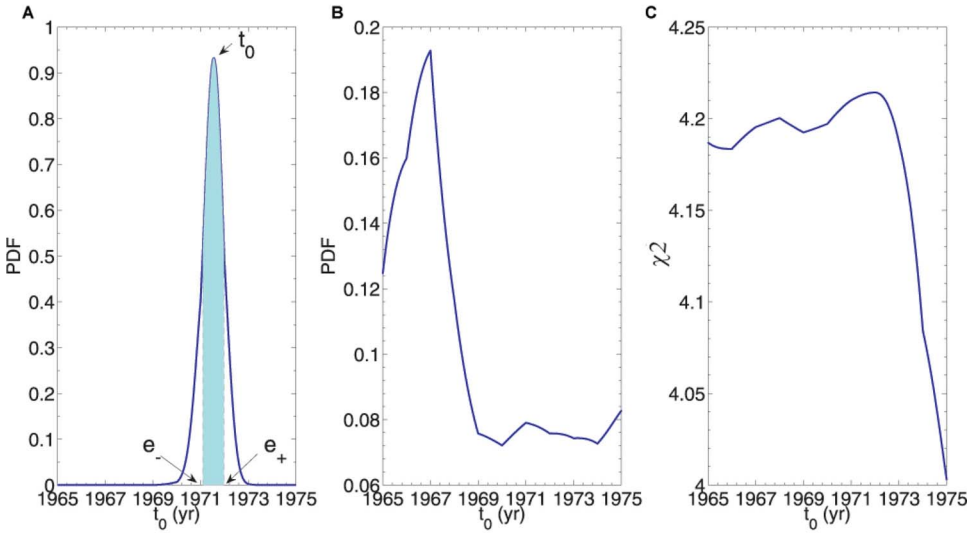

Figure 2. Examples of normalized probability distribution functions (PDFs) in (a) Gnangara observatory (GNA, *Y* component), (b) Port aux Francais observatory (PAF, *X* component), and (c) χ^2 curve of Vernadsky observatory (AIA, *Z* component) showing no minimum. The 1969 jerk was classified as detected (Figure 2a), excluded (Figure 2b), and not detected (Figure 2c).

[22] We make the assumption that the noise in the secular variation estimates obtained from annual means is uncorrelated, although this is not strictly the case, since the first difference of a time series has a covariance associated with it [*Haines*, 1993]. We find difficulties with this assumption for monthly mean data where a strong influence of temporally correlated external field variations remains. In order to correctly calculate error bars in t_0 for the monthly means, a more complex noise model that accounts for the time variations in the external field, should be adopted. Because of this limitation and due to more scatter being present in monthly mean secular variation estimates, we report error bars only for the case of annual means.

[23] Substituting the estimate of the data error bars (equation (6)) in the PDF (equation (5)):

$$prob(\mathbf{d}|t_0, \mathbf{m}, L_2) \propto \exp\left[-\frac{\chi^2(N-3)}{2\chi_m^2}\right], \qquad (8)$$

from which we evaluated the error bars in t_0 using 67% confidence interval. The jerks are classified as "not detected" when the minimum of the χ^2 curve (or maximum in the PDF curve) is at one of the extremes of the time interval studied. They are classified as "excluded" when it is not possible to obtain error bars because the 67% of the PDF area can not be completely calculated since much of the PDF is outside the time interval considered. Figure 2 illustrates examples where the jerk is classified as "detected" and the error bars can be calculated (Figure 2a); when it is not possible to calculate the error bars and the jerk is "excluded" (Figure 2b) and "not detected" when the minimum of the χ^2 curve is in one of the extremes, as shown in Figure 2c.

3.2. Spherical Harmonic Model for Jerk Amplitudes

[24] Jerk amplitudes are also measured at magnetic observatories and used to build global spherical harmonic models, assumed purely internal, where each component of the magnetic field presents a different jerk morphology ($\delta\ddot{X}(a, \theta, \phi)$, $\delta\ddot{Y}(a, \theta, \phi)$ and $\delta\ddot{Z}(a, \theta, \phi)$ for jerk amplitudes). These components are the gradients of the potential function ($\delta\ddot{V}$) associated with the jerk morphology, which can be expanded in spherical harmonics:

$$\delta\ddot{V}(a,\theta,\phi) = a\sum_{\ell=1}^{L}\sum_{m=0}^{\ell}\left(\frac{a}{r}\right)^{\ell+1}\left(\delta\ddot{g}_\ell^m\cos m\phi + \delta\ddot{h}_\ell^m\sin m\phi\right) \cdot P_\ell^m(\cos\theta)$$

where $\delta\ddot{g}_\ell^m$ and $\delta\ddot{h}_\ell^m$ are the Gauss coefficients (in nT/yr^2), r is the radius ($r = a$ is the Earth's radius, 6371.2 km), θ is the colatitude and ϕ the longitude. For each spherical harmonic model we calculate

the Lowes spatial spectrum at the Earth's surface [*Lowes*, 1966]:

$$\delta\ddot{R}_\ell = \left[(\ell+1)\sum_{m=0}^{\ell}\left[\left(\delta\ddot{g}_\ell^m\right)^2+\left(\delta\ddot{h}_\ell^m\right)^2\right]\right]. \quad (9)$$

[25] We solve the linear inverse problem of finding the Gauss coefficients given measurements of jerk amplitudes at different observatories. The data are weighted by their mean error bars calculated by $\frac{|e_{\min}|+|e_{\max}|}{2}$, where $e_{\min}$ and $e_{\max}$ are derived as follows:

[26] Our optimal value for $\delta\ddot{X}$ is that corresponding to our optimal choice of t_0 at that observatory. Then $e_{\max}$ and $e_{\min}$ are the differences from this value when the amplitude is found for the value of t_0 + $e_{\max}$ and t_0 + $e_{\min}$. In this way we discover how uncertainties map into imprecise values of the jerk amplitude estimate, thus supplying error bars.

[27] We apply the traditional regularization method of stabilizing the inversion [see, e.g., *Menke*, 1989; *Parker*, 1994; *Gubbins*, 2004] that involves minimizing a combination of solution norm ($\mathcal{N}$) and error or misfit (E):

$$T(\lambda) = E + \lambda\mathcal{N}, \quad (10)$$

where λ is called the trade-off or damping parameter which determines the relative importance of E and $\mathcal{N}$ [*Gubbins*, 2004]. We used the norm suggested by *Gubbins and Bloxham* [1985], to measure the spatial complexity of an internal potential field model, which in our notation is

$$\mathcal{N} = 4\pi\sum_{\ell,m}\left(\left(\delta\ddot{g}_\ell^m\right)^2+\left(\delta\ddot{h}_\ell^m\right)^2\right)\frac{(\ell+1)^2}{(2\ell+1)}\ell^3\left(\frac{a}{c}\right)^{2\ell}, \quad (11)$$

where c and a are the Earth's core and surface radius, respectively. We choose one of the candidate models at the knee of the trade-off curve ($\mathcal{N}$ versus E for each damping parameter λ) that represents a compromise between model complexity and misfit.

4. Results

4.1. Jerk Time Occurrence

[28] We applied our method of fitting two straight line segments to secular variation estimates derived from annual mean, monthly mean observatory data and annual mean synthetic data derived from the CM4 field model, using both L_2 and L_1 measures of misfit. Examples of the L_1 and L_2 fit to Fuerstenfeldbruck observatory data (Germany) and the corresponding misfit curve are shown in Figure 3. We found that the L_1 method shows no substantial discrepancies in the results of t_0 detection compared to the L_2 method: the patterns of late/early jerks are similar for both. The L_1 method would be advantageous only if there were many outliers in the data. Results for occurrence time and error bars, derived using the L_2 method, for the X, Y and Z components from the annual mean secular variation estimates, are shown in Tables A1–A4.

[29] In order to test different time windows for fitting the two straight lines, we choose five magnetic observatories (CLF, GNA, FRD, FUR and HLP) for X component, varying from 1963 to 1977 and from 1965 to 1975. We found that the occurrence times did not vary significantly (mean of 0.13 yr), but in some cases as GNA it is not possible to detected in the shorter time window, since t_0 = 1974. We decided to perform all the analysis for the 1969 jerk using the longer time window, approximately centered in each jerk occurrence time.

[30] We tested for the 1969 jerk, occurrence times were determined by the L_2 method using the first differences of annual mean data, first differences of 12 month running average of monthly means and the CM4 synthetic data. The results for the occurrence time (t_0) are again similar in all three data sets: the patterns of early/late jerks are consistent. The t_0 detected in CM4 model, considering only core contribution, showed more confidence (smaller error bars) compared to annual mean data (see Figures 4 and 5). The reason is that the synthetic CM4 data do not include external contributions, consequently jerks appear more clearly. However, the differences on the delay amplitudes and in the patterns early/late do not change significantly, showing that external fields affect mainly the error bars but not the overall analysis of jerks.

[31] In the reminder of the paper we prefer to analyze the first differences of annual mean data directly to determine the robustness of jerk occurrence times since the observatory annual means constitute the raw data that is better distributed than the monthly mean data. The main results for the jerks occurrence times are as follows:

[32] 1. The 1969 jerk (Figure 4) arrives earlier in European observatories compared to the ones in the Southern Hemisphere. However, in detail our results

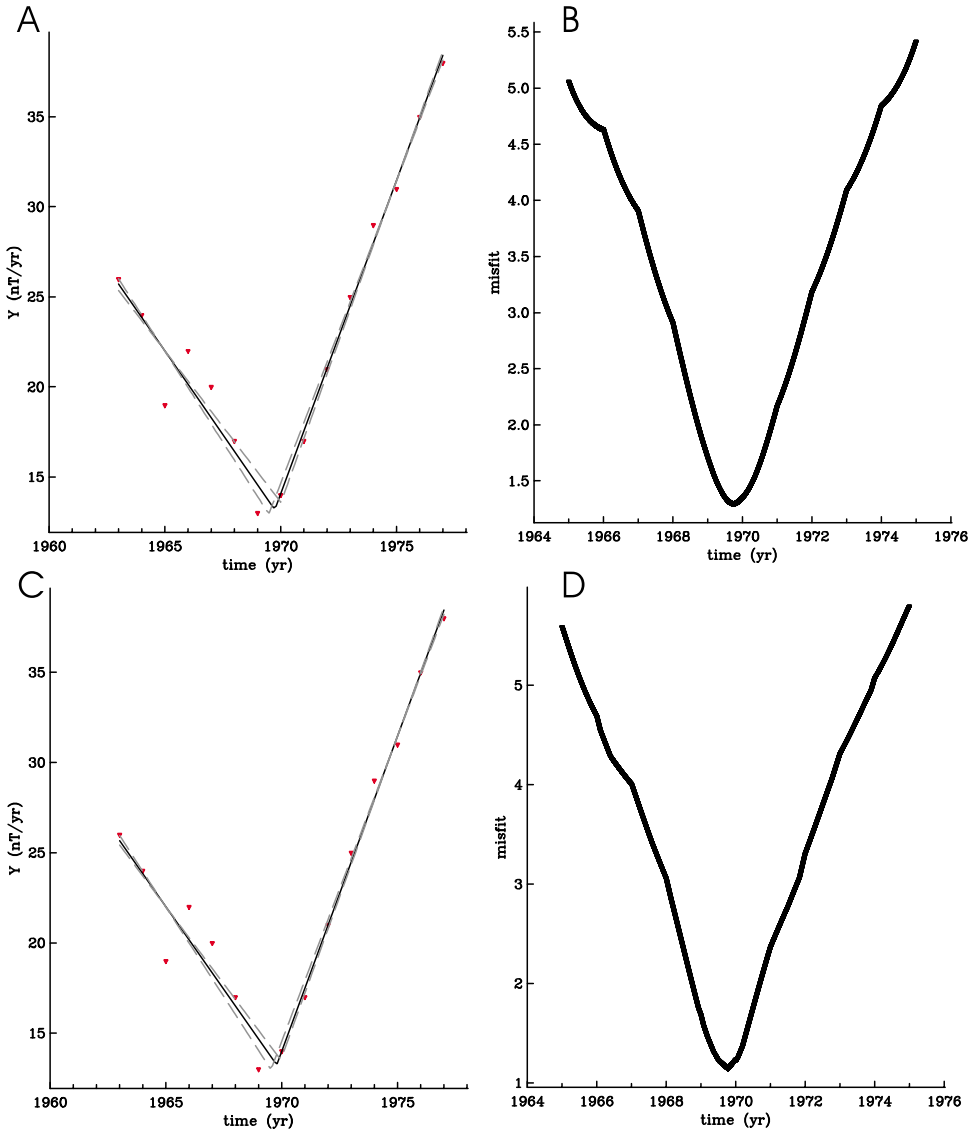

Figure 3. Example of (a) L_2 and (c) L_1 fitting of two straight line segments to the secular variation of Y component of Fuerstenfeldbruck observatory (FUR, Germany) obtained from first differences of observatory annual means and its associated misfit curve (in nT/yr) for (b) L_2 and (d) L_1. The solid line represents the minimum misfit chosen model, and the dashed lines represent the limits of the error bars (in Figures 3a and 3c).

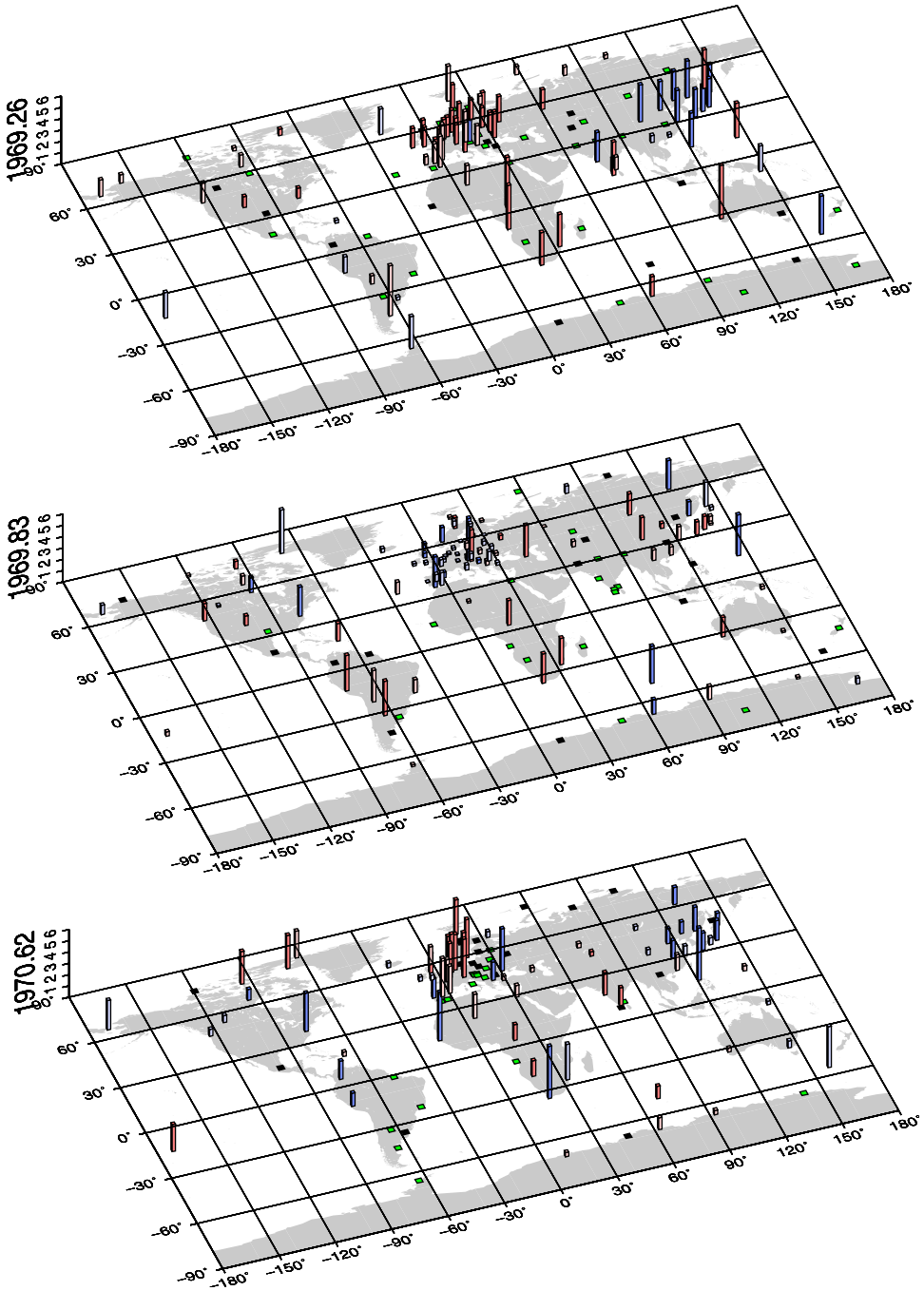

Figure 4. Results for the 1969 jerk occurrence time at the Earth's surface obtained by the L_2 method for the (top) X, (middle) Y, and (bottom) Z components of the magnetic field by considering first differences of observatory annual means. The mean occurrence time (e.g., 1969.94 for the X component) is shown close to the vertical bar (from 1 to 6 years) which gives the height of the blue and red bars. The red bars represent locations where the jerk appeared later than the mean occurrence time and the blue bars where it appeared earlier. The occurrence time when the bar is red is given by the sum of the mean occurrence time and the height of the bar in a specific location, while the occurrence time when the bar is blue is given by subtracting the mean occurrence time from the height of the bar. Dark red (blue) bars represent locations where the limits of the error bars are later (earlier) than the mean occurrence time and light red (blue) bars where the limits of the error bar are earlier (later). The green squares represent the locations where the jerk was not detected in the given component and the black squares where data were excluded.

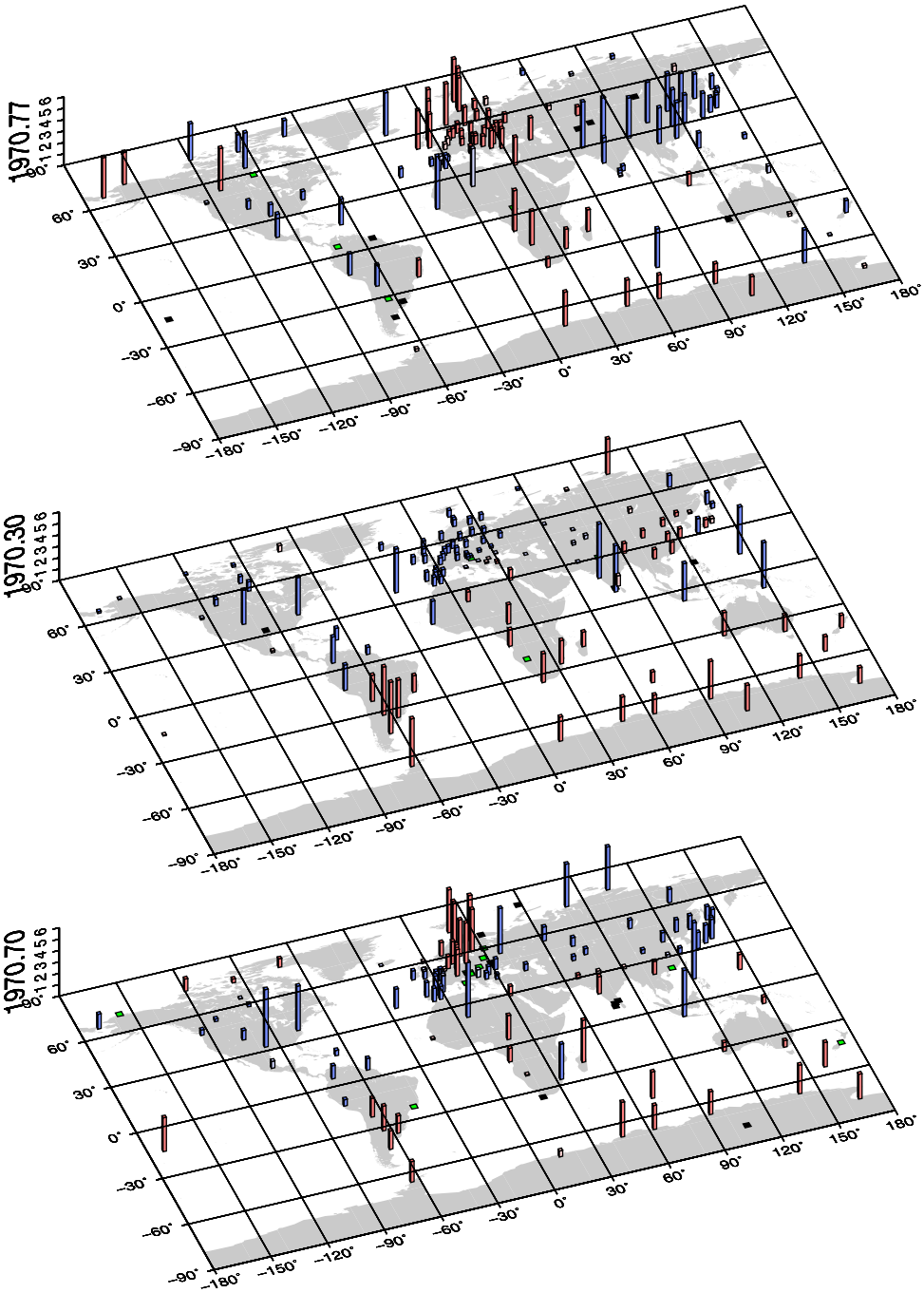

Figure 5. Results for the 1969 jerk occurrence time at the Earth's surface obtained by the L_2 method for the (top) X, (middle) Y, and (bottom) Z components of the magnetic field by considering first differences of the core magnetic field calculated by CM4. The labeling scheme is the same as in Figure 4.

show a more complex configuration with more geographical variation in the occurrence times; we found a pattern more complex than early in the north and late in the Southern Hemisphere as it is usually reported (see Figure 4, middle).

[33] 2. The 1978 jerk (Figure 6) shows early arrival of X component in the South East Asia region and late arrival of the Y component mostly in Europe, South Africa (3 observatories) and South America (2 observatories).

[34] 3. The 1991 jerk (Figure 7) is not observable in the X component across most of Europe and it occurred earlier in most of the US and in the Indian Ocean (3 observatories), while in the region around India (8 observatories) it arrived later. Conversely, in the Y component a later jerk is detected in North America and it is detected earlier in Europe.

[35] 4. The 1999 jerk (Figure 8) is not identified in our analysis. The most favorable result was in the X component, where it was possible to detect this jerk in 21 % of the observatories available, most of them being in Europe. Even on these few observatories the prominent change in slope did not appear clearly.

[36] The error bars for nearby European observatories in the analyzed jerks and in the three components mostly overlap (see, for example, Figures 9 (top), 9 (middle) and 9 (bottom)) demonstrating the consistency of our analysis. This overlapping is not expected in error bars of observatories in the Southern Hemisphere because they are not so close to each other. In general, the error bars of the jerk occurrence times turned out to be asymmetric ($e_- \neq e_+$) because of the asymmetric shape of the calculated PDF curves.

4.2. Jerk Morphology

[37] Jerk amplitudes were determined using the L_2 method applied to first differences of observatory annual mean data, for each magnetic component and for each jerk event. The patterns of positive and negative amplitudes are well defined, especially for the Y component.

[38] In Europe the 1969 jerk (Y component) intensities are positive while in Southern Hemisphere, North America, and in the Southeast Asian region the amplitudes are negative (Figure 10). In the subsequent 1978 jerk, the opposite pattern appeared: mostly positive amplitudes in North and South America and South East Asian region and negative in Europe and Africa (Figure 11) [see also *Le Huy et al.*, 1998].

[39] The jerk morphology in 1991 showed similar signs to the 1969 jerk, but with some differences for example at observatories in North America in which the amplitudes maintained positive in the X component (Figure 12, top). The amplitude range in the 1969, 1978 and 1991 jerks was about ± 15 nT/yr^2. The jerk amplitudes were found to be a more robust quantity than the jerk occurrence times, as illustrated by the small error bars (mean in the Y component of the 1969 jerk: $\sim \pm 0.41$ nT/yr^2).

[40] Using the amplitude measurements from magnetic observatories, we calculated global spherical harmonic models for the jerk amplitudes in the X, Y and Z components for each geomagnetic jerk. The spherical harmonic expansion is truncated at degree $L = 14$ and we explored the influence of varying a damping parameter on jerk morphology. Our preferred models avoid small scale structures in areas with few measurements. We tested different damping parameters (from $\lambda = 10^{-9}$ up to $\lambda = 10^{2}$) for the spherical harmonic models at the Earth's surface. We evaluated the Lowes spectra for each of the spherical harmonic models using these damping parameters.

[41] The trade-off curves for the 1969, 1978 and 1991 jerks suggest that damping parameters (λ) between 10^{-5} and 10^{-4} are the most appropriate since they are in the "knee" of the curve. We calculated the Lowes spectra for the three jerks spherical harmonic models (Figure 13) and found that they are similar for $\lambda = 10^{-5}$ and $\lambda = 10^{-4}$. We therefore chose to present only results of the spherical harmonic models for $\lambda = 10^{-5}$ for the 1969, 1978 and 1991 jerks (X, Y and Z components), shown in Figure 14.

5. Discussion

[42] The reasons why we choose annual mean values for the detection of geomagnetic jerks at magnetic observatories are (1) the annual mean data are less contaminated by the external field compared to the monthly means, which have higher noise levels in general (see Figure 1, for example), and (2) the annual mean data are more globally distributed than the available monthly mean data set [*Chulliat and Telali*, 2007].

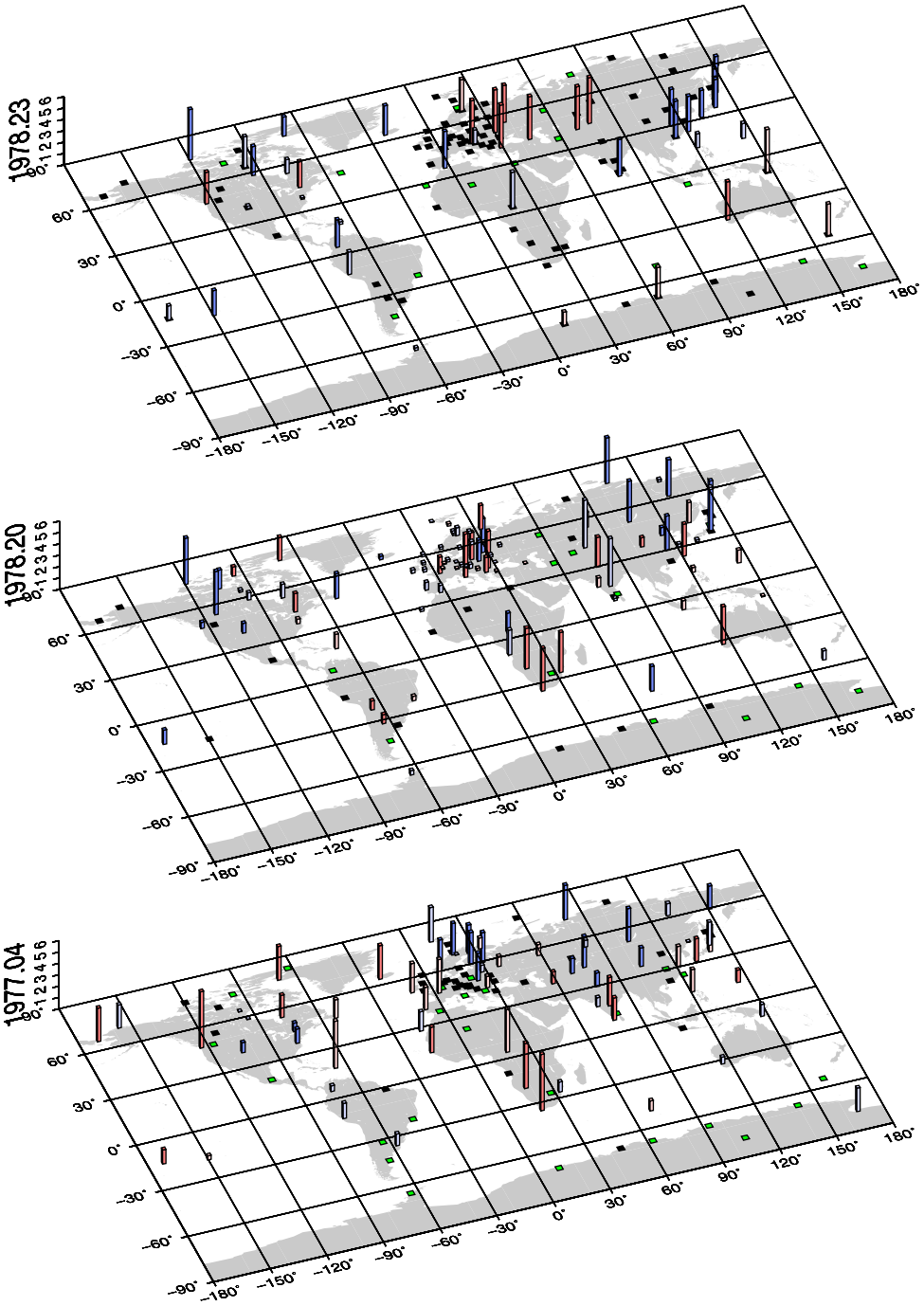

Figure 6. Results for the 1978 jerk occurrence time at the Earth's surface by the least squares method for the (top) *X*, (middle) *Y*, and (bottom) *Z* components of the magnetic field by considering first differences of observatory annual means. The labeling scheme is the same as in Figure 4.

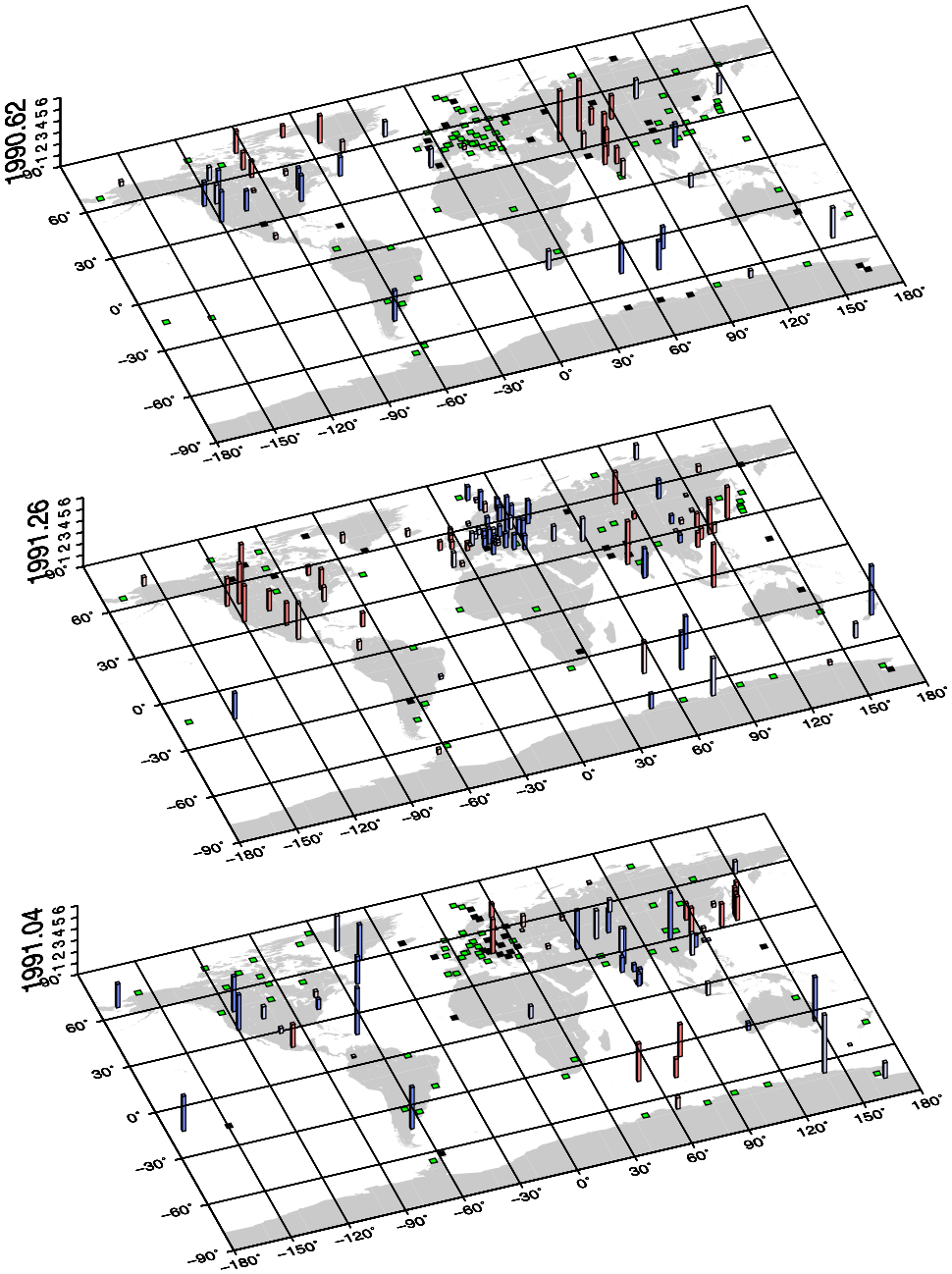

Figure 7. Results of the 1991 jerk occurrence time at the Earth's surface by the L_2 method for the (top) X, (middle) Y, and (bottom) Z components of the magnetic field by considering first differences of observatory annual means. The labeling scheme is the same as in Figure 4.

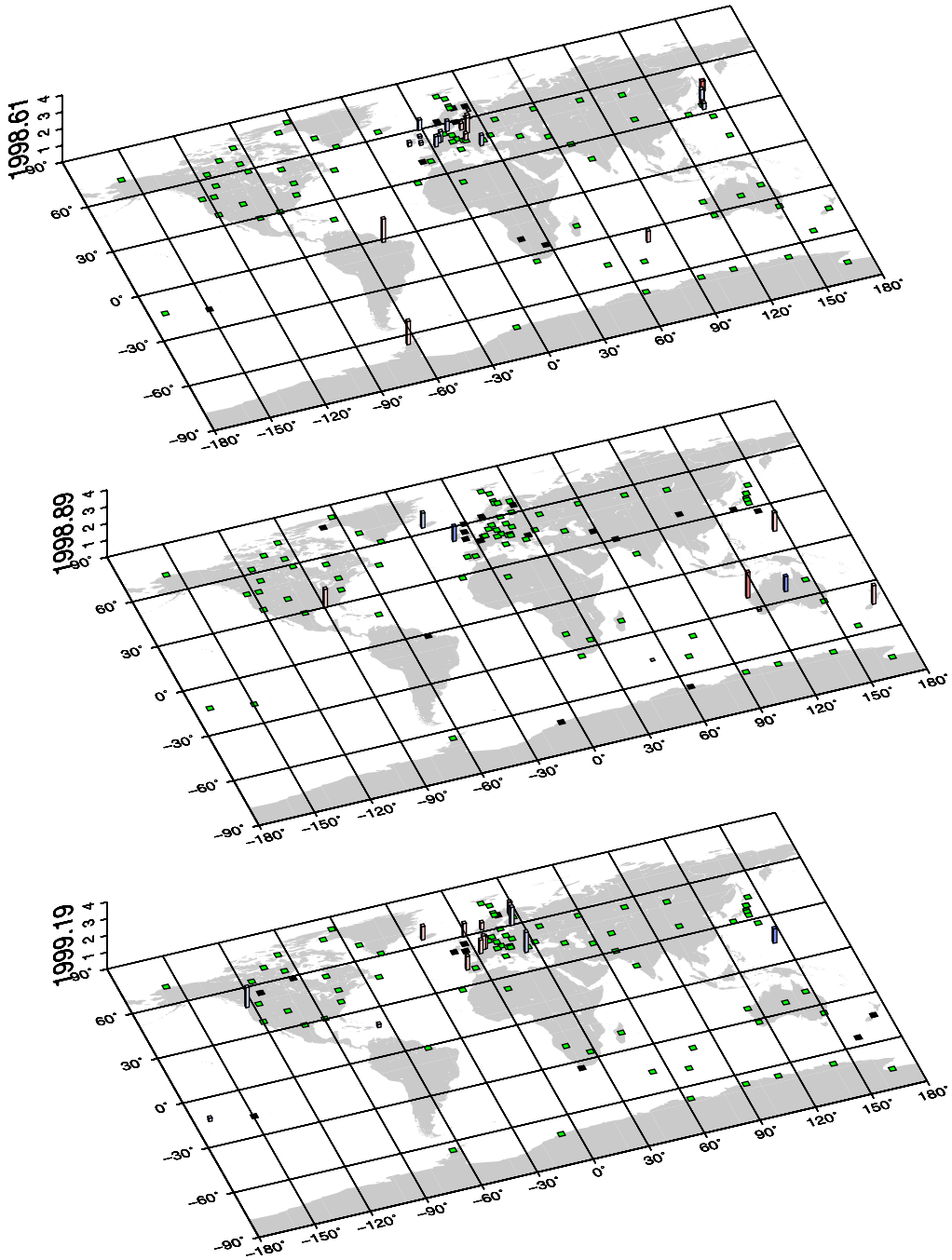

Figure 8. Results for the 1999 jerk occurrence time at the Earth's surface by the L_2 method to the (top) X, (middle) Y, and (bottom) Z components of the magnetic field by considering first differences of annual means. The labeling scheme is the same as in Figure 4.

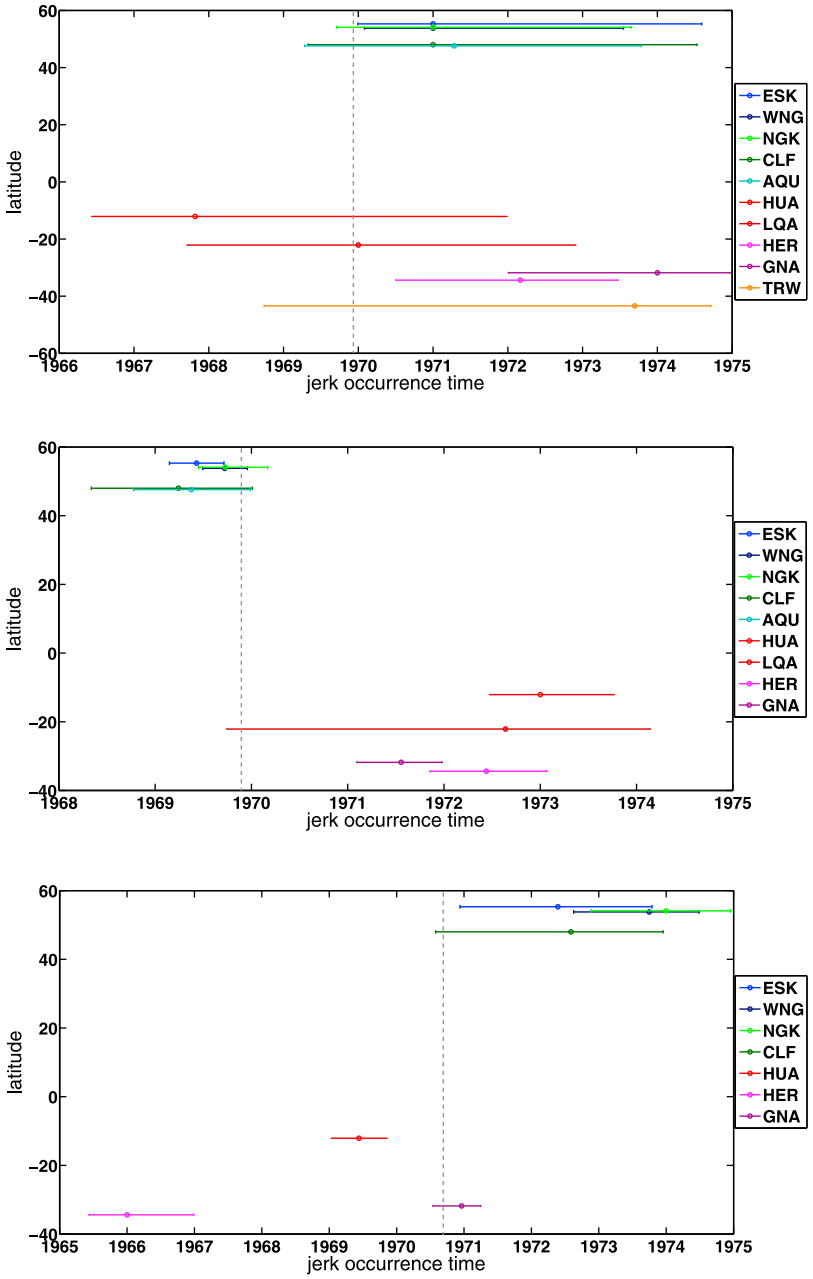

Figure 9. Error bars for the 1969 jerk occurrence time for a selection of magnetic observatories in the (top) X, (middle) Y, and (bottom) Z components of the magnetic field derived using first differences of annual means and the L_2 method. The observatories used as examples are Eskdalemuir (ESK, UK), Wingst (WNG, Germany), Niemegk (NGK, Germany), Chambon-la-Fôret (CLF, France), L'Aquila (AQU, Italy), Huancayo (HUA, Peru), La Quiaca (LQA, Argentina), Hermanus (HER, South Africa), Gnangara (GNA, Australia), and Trelew (TRD, Argentina).

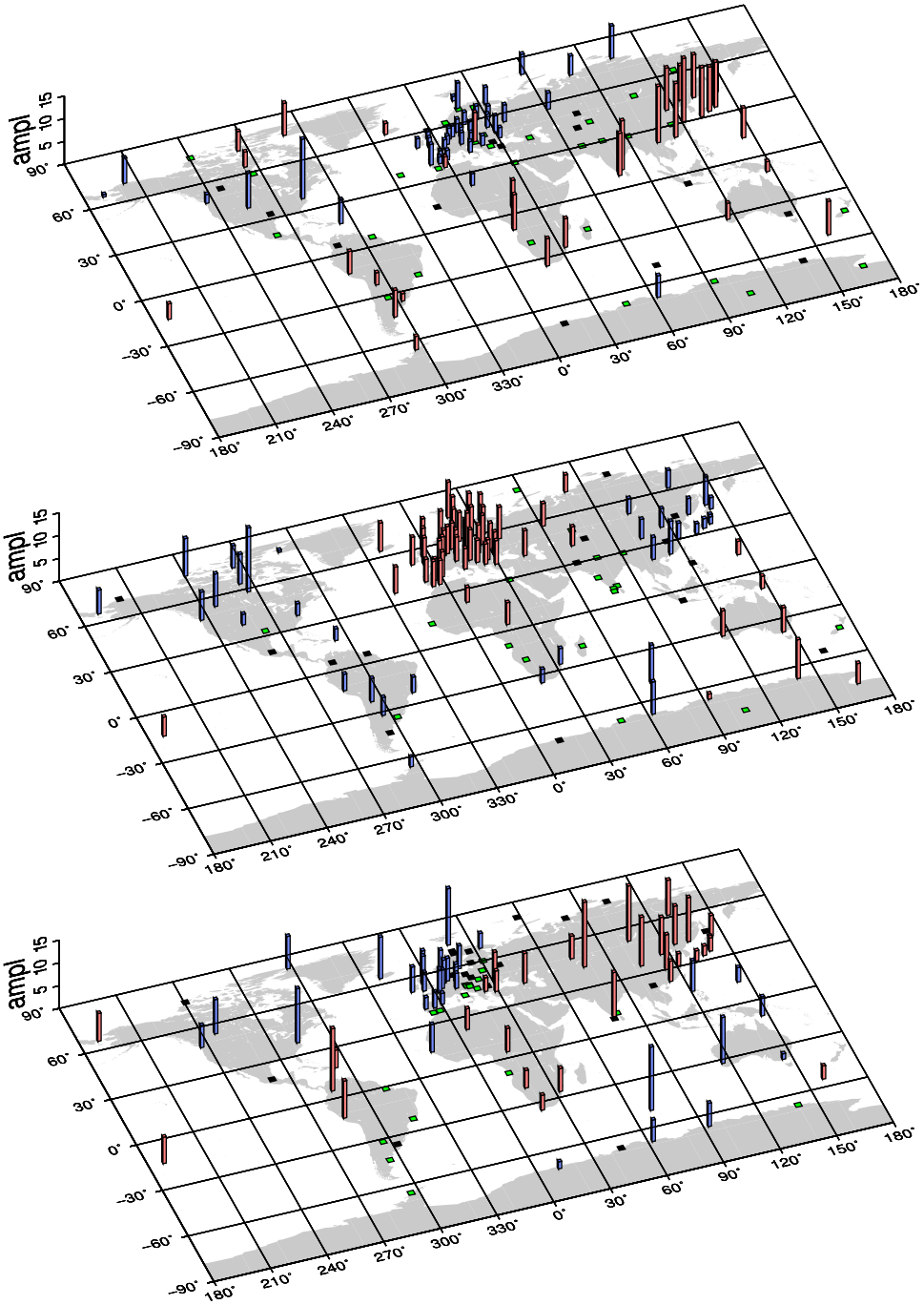

Figure 10. Jerk amplitudes (nT/yr^2) for the 1969 jerk detected by the L_2 method by using first differences of observatory annual mean data. The three maps displayed are the amplitudes of (top) X, (middle) Y, and (bottom) Z components. The red and blue bars represent negative and positive values of jerk amplitude, respectively.

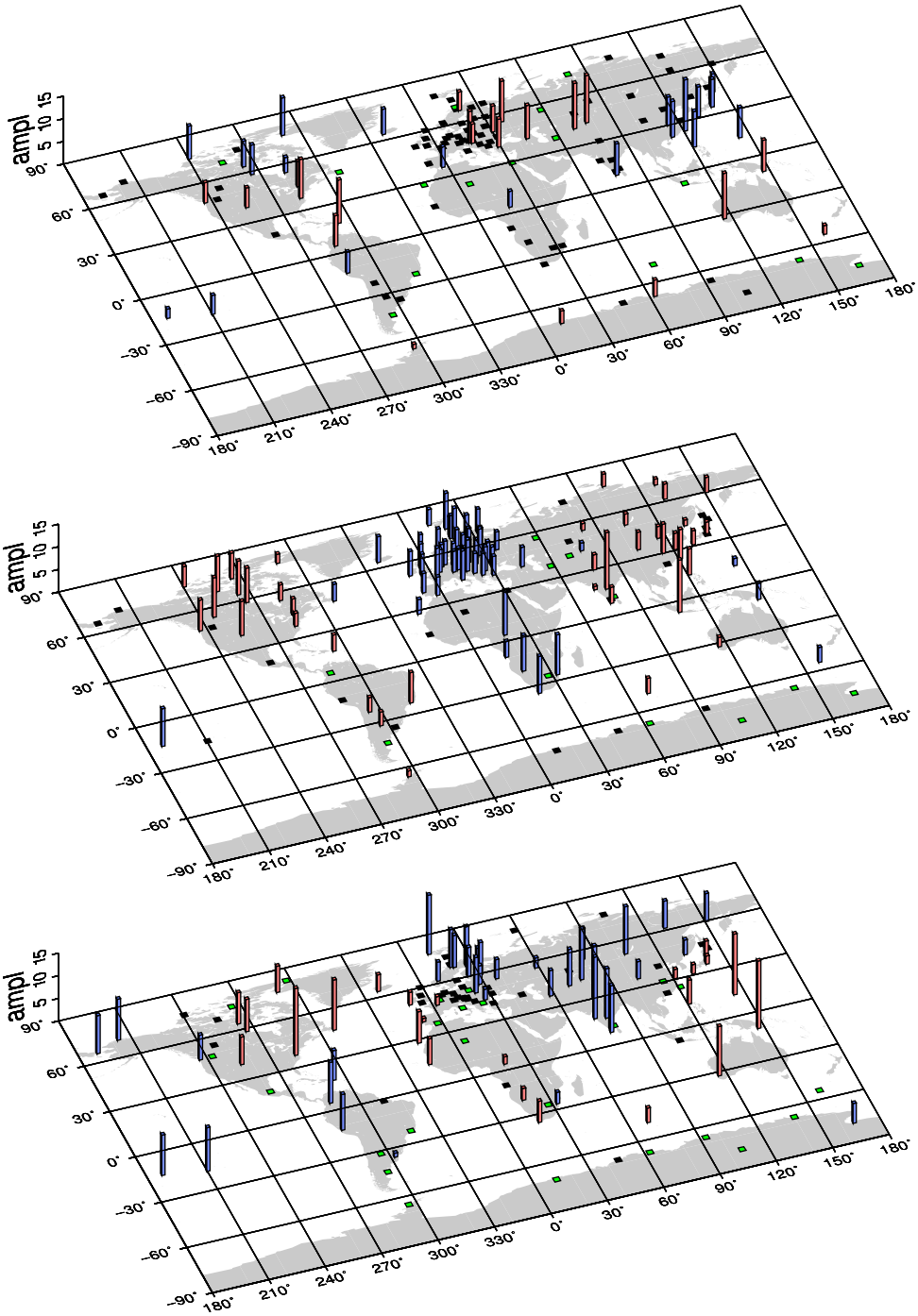

Figure 11. Jerk amplitudes (nT/yr^2) for the 1978 jerk detected by the L_2 method by using first differences of observatory annual mean data. The three maps displayed are the amplitudes of (top) X, Y, and (bottom) Z components. The labeling scheme is the same as in Figure 10.

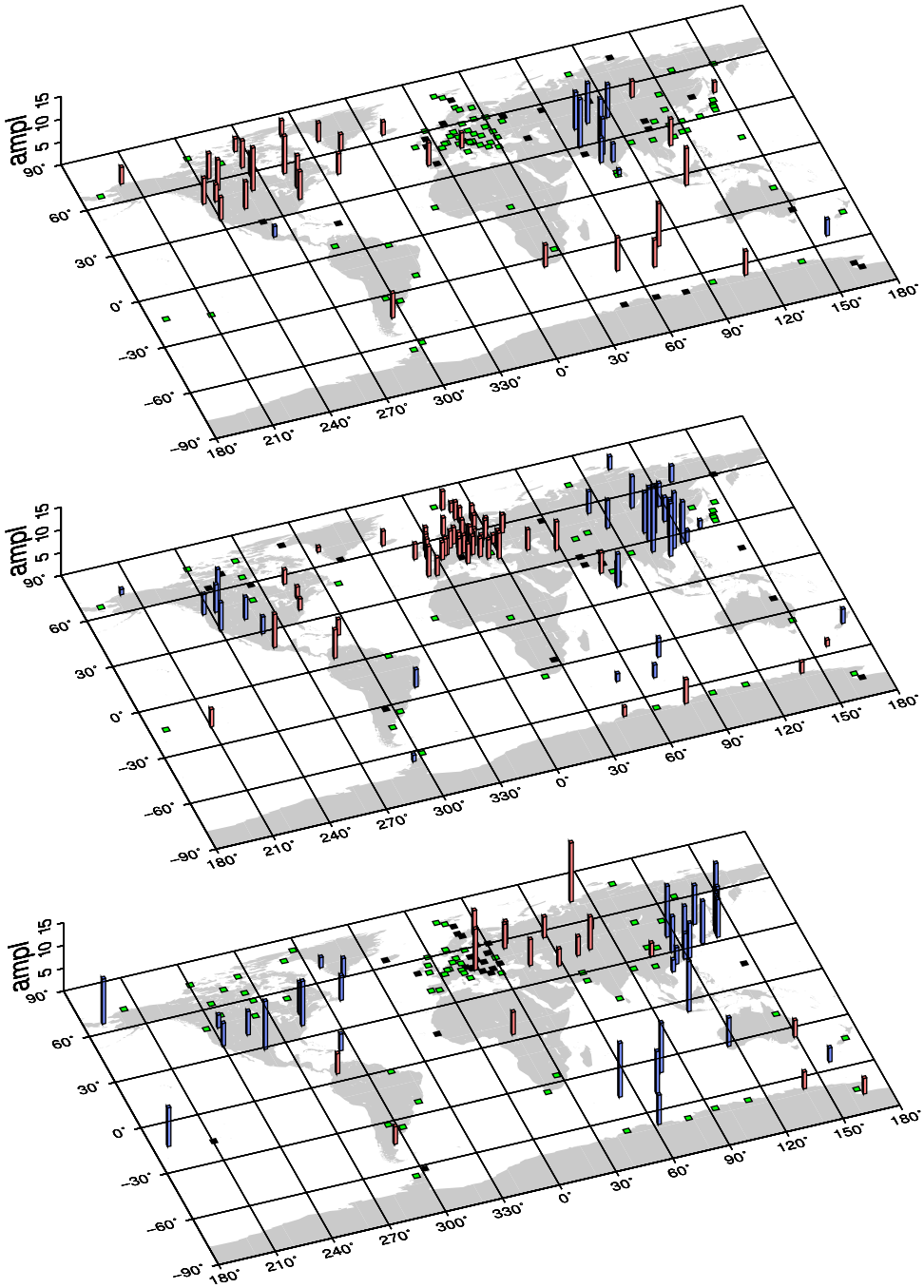

Figure 12. Jerk amplitudes (nT/yr^2) for the 1991 jerk detected by the L_2 method by using first differences of observatory annual mean data. The three maps displayed are the amplitudes of (top) X, (middle) Y, and (bottom) Z components. The labeling scheme is the same as in Figure 10.

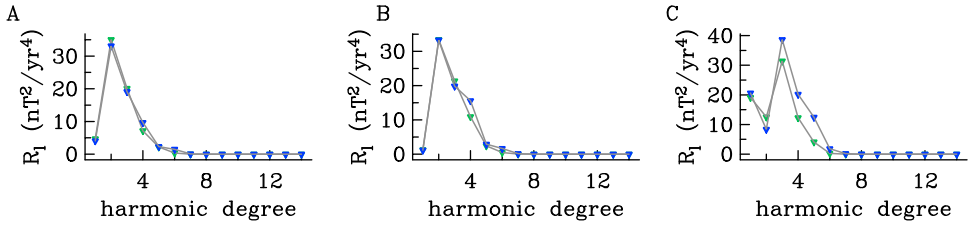

Figure 13. Lowes spectra of the (a) 1969, (b) 1978, and (c) 1991 spherical harmonic models using simultaneous analysis of the jerk amplitudes in X, Y, and Z components derived from L_2 analysis of first differences of observatory annual means for the damping parameters: $\lambda = 10^{-5}$ (blue triangles) and $\lambda = 10^{-4}$ (green triangles).

[43] Our results mostly corroborate those of *Nagao et al.* [2003] and *Chambodut and Mandea* [2005] who used monthly means and more sophisticated methods to detect jerks. However, we agree that monthly means may be more appropriate when analyzing rapid events such as the 2003 jerk, because more temporal resolution may be needed.

[44] Because the geographic distribution of magnetic observatories is uneven it is difficult to describe the global behavior of geomagnetic jerks; we therefore believe that when generalizing jerk global patterns, one should always mention the number of observatories in which any proposed jerk was detected. In addition, it is possible to analyze synthetic data evaluated by global field models (such as CM4) but one must also recognize that they are largely constrained by observatory data with nonuniform distribution.

[45] It is probable that our chosen model of two straight lines is too simple to represent jerks, but previous research using wavelet analysis and more complex statistical models are equally not based on any strong physical argument. All previous works, along with the present one, aim to find discontinuities in the secular variation, using different methodologies. The great advantage of our analysis is that we are able to estimate error bars, which are essential for (1) characterizing the patterns of early or late

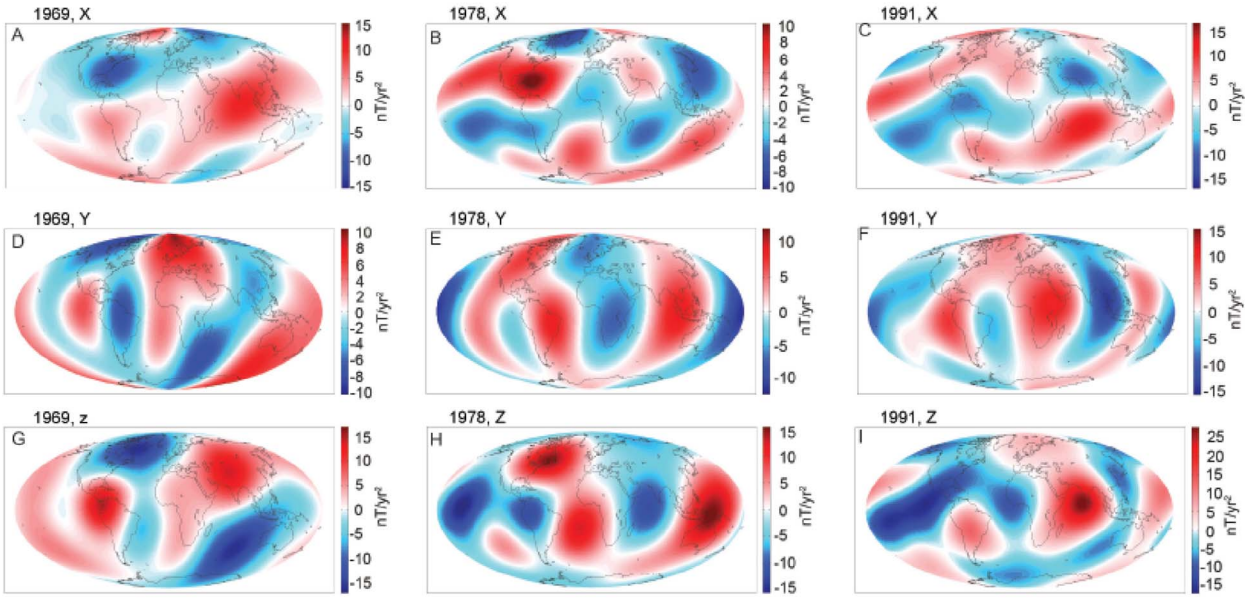

Figure 14. Spherical harmonic models of the 1969 jerk for the (a) X, (d) Y, and (g) Z components; of the 1978 jerk for the (b) X, (e) Y, and (h) Z components; and of the 1991 jerk for the (c) X, (f) Y, and (i) Z components using the damping parameters of $\lambda = 10^{-5}$.

occurrence times of geomagnetic jerks with a level of confidence and (2) enabling further studies relating jerks with mantle electrical conductivity.

[46] The results of jerk occurrence times in nearby observatories can be inconsistent by a few years in some regions such as in Europe for the *Y* component of the 1969 and 1978 jerks (Figures 4 and 6) and in North America for the *X* component for the 1978 jerk (Figure 6). Although the majority of the error bars overlap in nearby locations, it is possible that some large departures occur due to noise in the data. However, we should be careful not to rule out the possibility of early/late jerks in locations close to each other, because if one considers the hypothesis of jerk differential occurrence times generated totally by a conducting mantle it would be possible to generate these kinds of patterns depending on the mode mixing [*Pinheiro and Jackson*, 2008].

[47] The jerk amplitudes (in Figures 10 to 12) are more robust measurements than the occurrence times and there are only a few exceptions where there is a change in sign in observatories close to each other (e.g. Europe for the *X* component on the 1969 jerk) probably due to more influence of the external field in the data. However, note that such features are not represented in a regularized spherical harmonic models of jerk amplitudes (Figure 14).

[48] A summary of our results along with those obtained in previous studies is presented in Table A6. Concerning the 1969 jerk (*Y* component) our results mostly agree with *Nagao et al.* [2003] and *Chambodut and Mandea* [2005]: for example, in Europe the jerk appeared earlier and in the few observatories available in Africa and Australia, it appeared later with a time lag of about 3 years.

[49] The results of the 1978 also mostly agree with *Nagao et al.* [2003] and *Chambodut and Mandea* [2005]: South Africa and Australia have later jerks and in Western Africa we also found two observatories with an earlier arrival. *De Michelis and Tozzi* [2005] also analyzed the 1978 jerk and found a simpler pattern of early/late jerks that agrees mostly with *Nagao et al.* [2003] but disagree particularly in South America with *Chambodut and Mandea* [2005] and our results. In general, our calculated values of the mean error bars (Table A5) are larger than the ones estimated by *Alexandrescu et al.* [1996].

[50] The morphology found for the 1991 this jerk turned out to be more complicated than for previous jerks (1969 and 1978) and in all previous studies. In general, there is more disagreement between different works for the 1991 jerk as for example in Africa we were not able to detect the 1991 jerk while *Chambodut and Mandea* [2005] and *De Michelis et al.* [2000] found it to be earlier than the time inferred by *Nagao et al.* [2003].

[51] *Mandea et al.* [2000] were the first to mention the possible presence of a jerk at the end of the 20th century and detected visually the 1999 jerk in 9 observatories. *De Michelis and Tozzi* [2005] applied the traditional straight line fit to the monthly mean data for this jerk and claimed that the 1999 jerk could be identified in observatories in Europe, North America, Asia, Africa and the Pacific Ocean (total 29 out of 44 observatories). We believe that *DeMichelis and Tozzi*'s [2005] argument is not enough to classify the 1999 jerk as global; for example, the 1999 jerk was detected only in 4 observatories in the Southern Hemisphere, and the observatories where it was detected are mostly concentrated in Europe and North America. In addition, our results suggest that there is no global jerk in 1999 and in most of the few observatories where two straight lines could be fitted to the data, we found that the typical jerk "V" shape was not observed. It is also possible that the lower temporal resolution obtained using annual mean data make it more difficult to detect this jerk compared to monthly mean data.

[52] In relation to the jerk amplitudes our results can be compared to *Courtillot and Le Mouël* [1984] for the 1969 jerk, *Le Huy et al.* [1998] for all three jerks (1969, 1978 and 1991) and *De Michelis et al.* [2000] for the 1991 jerk. In general, our jerk morphology models are similar to the previous results. We found similar Lowes spectra as *Le Huy et al.* [1998] for the 1969 and 1978 jerks with a peak at $\ell = 3$ and for the 1991 jerk two peaks at $\ell = 1$ and $\ell = 3$ (Figure 13). The harmonic content of the jerk signal, which differs in the present work compared to the previous papers, will be crucial in our analysis of jerk observations to infer mantle electrical conductivity.

6. Conclusion

[53] The data analysis of geomagnetic jerks that are reported to have occurred in 1969, 1978, 1991 and 1999 has been performed using observatory annual mean data, observatory monthly mean data and the

core contribution calculated from the CM4 model. Two methods of fitting straight lines to the secular variation were applied using L_1 and L_2 norm measures of misfit. It was expected that the L_1 approach would allow a better fit to the observatory data since it is not as sensitive to noise and outliers as the L_2 method. However, analysis of the 1969 jerk showed that there are only small differences between the two methods and that there is not much advantage in applying the more expensive L_1 method instead of L_2 method. Since jerk time delays obtained from the annual means data, monthly means data and the CM4 model showed similar patterns, we presented in detail only results of the L_2 method applied to the first differences of observatory annual means.

[54] The analysis of error bars in the occurrence time of geomagnetic jerks proved to be essential in order to reliably distinguish between early and late jerk occurrences. In general, the error bars in t_0 were smaller in the Y component than in the X and Z components. The 1969, 1978 and 1991 jerks were detected worldwide in the secular variation estimates derived from annual means, while the proposed event in 1999 was detected only locally. The nonsimultaneous behavior of geomagnetic jerks presented a different pattern for each magnetic component and for each jerk event. Our analysis showed that the error bars for the Y component are in general smaller than in the X and Z components, probably due to a smaller influence of external field variations, therefore we can more confidently describe the nonsimultaneous behavior in the Y component. In general, the Southern Hemisphere observatories presented larger error bars.

[55] Instead of a general description of late in the Southern Hemisphere and early in the Northern Hemisphere, our analysis showed a more complex pattern with generally early arrivals in Europe and later arrivals in South America and Africa (both have few observatories available) in the Y component of the 1969 jerk. Conversely, in the X and Z components a later arrival of the 1969 jerk appeared in Europe and Africa and mostly early occurrences were found in South America. In the Y component of the 1978 jerk we found a late time occurrence in most of Europe and South Africa and for the same component of the 1991 jerk we observed an early arrival in Europe and a late arrival in North America and South East Asia.

[56] The patterns of positive/negative jerk amplitudes were better defined in the Y component and at most locations presented opposite signs in consecutive jerks. The amplitude measurements were used to build spherical harmonic models. By using different damping parameters we evaluated the trade-off curve for each geomagnetic jerk, in order to choose the most appropriate models for the jerk morphology. The chosen models in all three jerks to have the damping parameter value of $\lambda = 10^{-5}$ and power spectra that vanish at harmonic degrees are above five ($L = 5$) for the 1969 and 1978 jerks and above six ($L = 6$) for the 1991 jerk. The strongest peaks in the power spectra for the 1969 and 1978 jerks are at $\ell = 2$ while for the 1991 jerk the strongest peak is found at $\ell = 3$.

[57] The jerk data analysis, including error estimates, presented here can be used in the future to provide new constraints on the properties and dynamical processes occurring in the Earth's deep interior, with particular importance for estimates of the electrical conductivity of the mantle and for the possible mechanisms generating geomagnetic jerks. One possible way to explain the geomagnetic jerk time delay patterns is by considering a 1D electrically conducting mantle and the morphologies that vary for each magnetic component and each magnetic jerk. *Pinheiro and Jackson* [2008] demonstrated that even by assuming a simple model of a radial conducting mantle and the effects of some harmonic mixing (varying for each jerk and component) it is possible to generate differential jerk occurrence times. Since deep mantle electrical conductivity is poorly known, in a future study we will attempt to solve the inverse problem of determining mantle electrical conductivity from jerk differential occurrence times, using the associated error bars as estimated in this paper.

Appendix A

[58] The results of occurrence dates and the error bars of the 1969, 1978, 1991 and 1999 geomagnetic jerks for the X, Y and Z components are shown in Tables A1–A4, respectively. The number of observatories included and excluded and the ones in which jerks were not detected are presented in Table A5. A summary of previous work on the detection of geomagnetic jerks is shown in Table A6.

Table A1. Occurrence Date (τ) of the 1969 Geomagnetic Jerk in the Annual Means of the X, Y, and Z Components of Each Magnetic Observatory[a]

	X			Y			Z		
Observatory	τ	e_-	e_+	τ	e_-	e_+	τ	e_-	e_+
AAA	◇			×			1971.0	−0.4	0.2
ABG	1966.7	−0.5	0.9	◇			1972.6	−1.3	0.8
ABK	◇			1970.8	−0.8	0.7	×		
AIA	1966.4	−1.3	4.7	1970.0	−0.7	2.2	◇		
ALE	*			*			1973.0	−6.4	0.2
ALM	1972.0	−4.1	2.0	1968.7	−0.7	1.6	◇		
AML	◇			◇			*		
ANN	1970.4	−2.0	1.1	◇			◇		
API	1967.0	−1.4	5.3	1970.2	−2.0	1.4	1973.0	−0.3	0.6
AQU	1971.3	−2.0	2.5	1969.4	−0.6	0.6	◇		
BEL	*			*			×		
BJI	1966.7	−0.7	0.6	1970.3	−0.4	0.5	1969.3	−0.5	0.5
BJN	1972.4	−5.6	0.8	1970.0	−0.4	0.4	1973.7	−1.4	1.3
BLC	1970.3	−1.6	3.1	1970.6	−1.5	1.7	1969.7	−0.8	0.8
BNG	1973.7	−2.0	1.0	1972.0	−1.0	2.9	1972.0	−1.4	1.9
BOU	1970.2	−0.7	0.7	1970.7	−0.7	0.5	*		
BRW	1970.0	−1.1	1.1	×			*		
CCS	1969.6	−0.6	0.6	×			×		
CLF	1971.0	−1.7	3.5	1969.2	−0.9	0.8	1972.6	−2.0	1.4
CNH	1966.7	−1.0	1.0	×			1969.6	−0.7	0.7
COI	1970.0	−1.1	0.9	1969.8	−0.4	0.6	1968.9	−2.4	1.3
CPA	1968.7	−2.0	3.5	1970.8	−1.4	2.5	×		
CWE	1970.8	−3.3	3.4	1969.0	−0.6	5.6	1968.0	−0.7	3.8
DAL	×			◇			*		
DIK	1970.0	−1.4	1.2	1969.2	−1.8	1.9	×		
DOB	◇			1968.5	−0.5	0.6	1972.5	−0.8	1.8
DOU	1971.0	−2.1	2.6	1969.6	−0.4	0.4	1973.6	−1.4	0.9
DRV	×			1970.0	−1.3	2.0	◇		
EBR	1971.0	−2.5	2.9	1969.3	−0.5	0.4	1973.0	−4.1	0.7
ESK	1971.0	−1.0	3.6	1969.4	−0.3	0.3	1972.4	−1.5	1.4
FCC	◇			1968.5	−0.4	1.3	*		
FRD	1970.2	−0.4	0.5	1967.3	−0.7	0.7	1967.2	−0.7	0.5
FUQ	×			×			1969.0	−1.2	1.3
FUR	1971.0	−1.3	1.8	1969.7	−0.3	0.3	1974.0	−0.8	0.7
GCK	1971.0	−1.8	2.4	1969.5	−0.3	0.3	◇		
GNA	1974.0	−2.0	1.0	1971.6	−0.5	0.4	1971.0	−0.4	0.3
GUA	1972.3	−1.1	1.4	1966.2	−1.0	0.8	1971.1	−0.8	2.3
GZH	1969.0	−1.9	1.4	1970.6	−2.4	3.4	1972.0	−1.7	1.0
HAD	1971.0	−1.6	2.2	1969.6	−0.3	0.3	1970.2	−0.6	2.3
HER	1972.2	−1.7	1.3	1972.4	−0.6	0.6	1966.0	−0.6	1.0
HIS	1970.0	−0.8	1.6	◇			×		
HLP	1971.0	−2.1	1.8	1970.4	−1.0	0.5	×		
HRB	1966.5	−1.0	1.0	1969.3	−1.1	1.2	◇		
HUA	1967.8	−1.4	4.2	1973.0	−0.5	0.8	1969.4	−0.4	0.4
IRK	◇			1971.7	−1.1	0.5	1970.3	−0.6	0.5
ISK	×			1969.6	−0.7	0.8	1971.0	−2.4	1.3
KAK	1967.0	−0.8	0.7	1970.5	−0.7	0.6	1969.0	−0.6	0.4
KGD	×			◇			1971.0	−1.2	1.1
KIV	1971.0	−0.6	0.8	1969.5	−0.3	0.4	*		
KNY	1966.8	−0.5	0.6	1971.0	−0.7	0.6	1969.1	−0.7	1.0
KNZ	1966.7	−0.6	0.6	1970.0	−1.0	1.3	1968.9	−0.5	0.4
KOD	1970.5	−1.2	1.5	◇			1972.2	−0.6	1.1
LAS	1969.0	−1.2	5.3	◇			×		
LER	×			1969.3	−0.4	0.4	1972.2	−2.4	0.8
LGR	1971.0	−1.7	0.8	×			*		
LMM	1972.1	−1.1	1.7	1972.2	−1.3	1.4	1967.5	−2.2	3.2
LNN	1971.5	−1.0	2.5	1969.8	−0.4	0.3	◇		
LOV	1971.1	−0.9	2.2	1969.8	−0.3	0.3	1974.0	−0.7	0.8
LQA	1970.0	−2.3	2.9	1972.6	−2.9	1.5	*		
LRV	1967.0	−1.5	4.1	1969.5	−0.4	0.4	1970.2	−0.8	1.4

Table A1. (continued)

	X			Y			Z		
Observatory	τ	e_-	e_+	τ	e_-	e_+	τ	e_-	e_+
LSA	◇			◇			*		
LUA	1973.2	−3.2	1.2	◇			◇		
LVV	◇			1970.2	−0.6	0.3	◇		
LZH	1966.0	−0.4	0.4	1971.8	−0.4	0.6	1970.1	−0.8	0.7
MAW	1971.0	−0.8	1.9	1968.5	−1.0	0.9	1971.7	−2.6	3.2
MBC	◇			1970.0	−0.5	0.5	×		
MBO	×			◇			1966.3	−0.4	1.6
MCQ	1965.9	−0.6	0.7	×			1967.0	−1.4	5.2
MEA	×			1969.7	−0.5	0.5	1970.0	−0.9	0.8
MIR	◇			1971.0	−5.0	1.0	1971.0	−1.5	3.7
MLT	◇			◇			1971.6	−4.4	1.7
MMB	1966.8	−1.0	0.7	1969.6	−0.6	0.6	1969.5	−0.4	0.4
MMK	1970.0	−0.9	1.5	1970.0	−1.0	0.8	1970.1	−2.8	2.5
MNK	1971.0	−1.4	2.0	1969.5	−0.7	1.0	◇		
MOL	◇			◇			×		
MOS	1971.5	−0.8	1.9	1970.2	−0.3	0.4	×		
MUT	1966.3	−0.7	1.3	×			1966.0	−0.4	0.7
NCK	◇			1966.1	−0.7	0.5	◇		
NGK	1971.0	−1.3	2.7	1969.7	−0.3	0.4	1974.0	−1.1	1.0
NUR	1971.0	−0.9	2.3	1969.6	−0.2	0.2	×		
NVL	×			×			1971.0	−3.9	2.8
ODE	1971.6	−1.5	3.2	1970.1	−0.6	0.4	1966.9	−1.0	1.0
PAB	◇			×			*		
PAF	×			1966.5	−0.5	0.7	1971.7	−0.3	0.2
PAG	◇			1970.2	−0.6	0.5	1969.0	−1.9	1.2
PIL	◇			1972.9	−2.2	1.6	◇		
PMG	1967.0	−0.9	4.6	1970.1	−1.6	0.9	1970.3	−2.8	2.4
QUE	◇			×			*		
RES	1969.5	−2.4	1.5	1970.5	−0.5	0.5	1973.5	−0.6	0.5
RSV	1971.2	−0.8	1.8	1969.6	−0.4	0.5	×		
SAB	◇			◇			*		
SBA	◇			1969.3	−1.1	1.3	*		
SFS	◇			1967.1	−1.5	1.9	◇		
SJG	1969.0	−0.8	0.3	1971.4	−1.0	0.6	1971.0	−2.0	2.0
SMG	◇			1970.9	−1.9	0.5	*		
SOD	◇			1969.6	−0.3	0.3	×		
SSH	1966.5	−0.3	0.4	1971.0	−1.3	0.6	1969.8	−3.2	1.5
SSO	1967.0	−0.7	1.0	1971.0	−1.0	1.0	1970.0	−2.1	0.9
SUA	×			1969.0	−0.8	1.4	×		
SVD	1971.0	−1.3	0.8	1969.9	−0.4	0.2	*		
TAM	1971.0	−2.7	3.6	1970.0	−3.6	3.0	1972.7	−2.2	1.6
TAN	◇			◇			*		
TEO	◇			×			×		
TFS	◇			1972.6	−0.7	1.2	1971.0	−1.8	0.8
THL	1969.8	−0.4	0.6	1966.0	−1.0	5.7	1973.6	−1.3	0.7
THY	◇			1972.6	−1.8	0.9	◇		
TKT	×			1970.3	−0.7	0.4	*		
TNG	×			×			*		
TOL	1971.0	−2.4	3.4	1969.2	−0.6	0.8	1974.0	−4.0	0.6
TOO	×			1970.0	−0.5	0.9	1970.0	−3.8	1.8
TRD	1972.2	−0.7	0.8	◇			×		
TRO	1971.4	−1.2	1.5	1969.4	−0.5	0.5	×		
TRW	1973.7	−5.0	1.0	×			◇		
TSU	◇			◇			1972.0	−0.5	0.5
TTB	*			*			◇		
VAL	1971.0	−1.4	2.7	1969.6	−0.2	0.2	1970.2	−0.8	1.3
VIC	1971.0	−2.5	2.2	1971.4	−0.7	0.4	1970.0	−0.9	2.2
VLA	1966.0	−0.4	0.6	1968.6	−0.8	0.7	1968.5	−1.7	1.5
VOS	◇			◇			*		
VSS	◇			1971.0	−2.7	0.6	◇		
WHN	◇			×			1969.0	−2.3	1.6

Table A1. (continued)

Observatory	X			Y			Z		
	τ	e_-	e_+	τ	e_-	e_+	τ	e_-	e_+
WIK	1971.0	−2.4	1.9	1969.5	−0.3	0.3	◇		
WIT	1971.0	−1.7	2.3	1969.8	−0.2	0.2	1974.0	−1.5	0.9
WNG	1971.0	−0.9	2.6	1969.7	−0.2	0.2	1973.8	−1.1	0.7
YAK	◇			1967.3	−1.2	1.5	1969.1	−1.0	1.2
YSS	1972.7	−2.0	1.2	1967.7	−1.2	2.1	×		

[a]Detected by fitting two straight-line segments to data in the least squares sense. Symbols: diamond, observatories where the jerk was not detected; cross, observatories excluded when the minimum of the misfit curve is in one of the extremities; asterisk, observatories excluded when there was not enough data to perform the analysis. The left and right limits of 67% confidence are given by e_- and e_+, respectively.

Table A2. Occurrence Date (τ) of the 1978 Geomagnetic Jerk[a]

Observatory	X			Y			Z		
	τ	e_-	e_+	τ	e_-	e_+	τ	e_-	e_+
AAA	*			1974.0	−0.8	5.5	1974.3	−0.9	0.5
ABG	×			1979.0	−4.8	1.6	1976.3	−0.5	2.4
ABK	×			1978.0	−0.2	0.4	1974.3	−0.8	2.4
AIA	1978.0	−0.7	1.9	1977.8	−1.4	0.9	*		
ALE	*			*			◇		
ALM	*			1977.6	−1.2	1.0	◇		
ANN	×			◇			◇		
API	1977.0	−2.9	3.4	1977.0	−0.6	0.5	1978.3	−0.6	0.6
AQU	×			1982.0	−3.7	0.8	◇		
ARS	◇			◇			1978.0	−1.3	0.9
ASH	◇			◇			1978.1	−0.6	0.7
BDV	×			1978.0	−0.3	0.6	×		
BEL	×			1980.6	−1.5	0.7	◇		
BJI	×			1977.5	−1.1	0.6	×		
BJN	×			1978.4	−0.5	0.5	×		
BLC	1975.5	−1.3	3.8	1978.0	−0.6	0.7	1977.0	−0.9	2.6
BNG	1975.1	−1.3	4.6	1976.5	−1.7	0.9	1980.8	−6.0	0.6
BOU	1978.0	−0.9	3.1	1977.3	−0.5	0.4	1976.2	−1.0	0.9
BRW	×			×			1975.0	−2.0	4.4
CBB	◇			1976.5	−0.5	0.8	◇		
CCS	×			1974.2	−1.0	2.7	×		
CLF	×			1979.7	−0.4	0.4	1980.0	−4.6	1.0
COI	×			1977.5	−0.9	0.7	1979.0	−4.1	2.5
CWE	×			×			1980.0	−2.6	0.7
DIK	◇			×			1974.0	−0.6	0.7
DOB	×			1978.0	−0.4	0.3	1974.5	−1.5	1.5
DOU	×			1978.3	−0.5	0.5	◇		
DRV	◇			◇			◇		
ESK	×			1978.0	−0.4	0.3	×		
FCC	*			1977.6	−2.3	0.7	1977.0	−1.3	2.2
FRD	*			1978.6	−1.5	0.8	1975.8	−0.5	0.7
FUQ	*			◇			1976.5	−1.4	2.5
FUR	×			1978.3	−0.4	0.5	×		
GCK	×			1978.4	−0.5	0.7	×		
GNA	*			1981.5	−2.8	1.5	1976.4	−0.6	0.7
GUA	*			1979.3	−2.4	1.1	1978.1	−0.4	0.2
GWC	1977.0	−0.7	1.9	1977.0	−1.0	1.7	1979.0	−1.4	0.9
GZH	*			×			×		
HAD	×			1977.9	−0.4	0.3	×		
HBK	×			◇			*		
HER	×			1982.0	−0.4	0.5	1982.0	−0.9	0.8
HIS	*			*			×		
HLP	×			1979.9	−1.7	1.0	×		
HRB	×			1978.1	−0.4	0.6	×		

Table A2. (continued)

	X			Y			Z		
Observatory	τ	e_-	e_+	τ	e_-	e_+	τ	e_-	e_+
HUA	*			×			1975.7	−0.8	1.4
HYB	×			1974.0	−0.9	5.7	1979.6	−1.8	0.6
IRK	×			1974.6	−1.5	3.0	1974.1	−0.8	1.6
ISK	*			1978.3	−1.1	1.6	×		
KAK	*			1973.8	−0.8	2.6	1979.0	−3.2	1.6
KGD	×			×			×		
KIR	1981.0	−3.2	1.7	1977.5	−0.7	0.8	1977.0	−2.1	0.9
KIV	*			1978.0	−0.4	0.9	×		
KNY	*			1978.0	−0.5	0.5	1979.1	−1.3	1.3
KNZ	*			×			1979.4	−2.9	1.3
KOD	×			×			1975.7	−1.2	0.8
LAS	×			×			1976.0	−2.8	3.6
LER	×			1978.0	−0.4	0.4	×		
LMM	×			1981.7	−0.5	0.5	1976.2	−2.9	1.4
LNN	×			1978.3	−0.4	0.5	1974.4	−1.3	2.4
LNP	*			1981.0	−2.1	0.5	◇		
LOV	×			1978.0	−0.2	0.4	×		
LQA	×			1979.0	−0.7	1.1	*		
LRV	*			1977.9	−0.5	0.3	1980.0	−2.8	2.0
LUA	×			1976.0	−2.9	2.5	×		
LVV	×			1976.3	−0.7	0.6	1974.6	−0.8	0.6
LZH	×			1979.0	−0.5	0.5	1975.4	−1.0	1.3
MAW	1980.9	−4.2	1.6	◇			◇		
MBC	*			1974.1	−0.9	3.7	×		
MBO	×			×			1979.3	−1.4	1.3
MCQ	1981.0	−5.3	1.1	1977.4	−2.9	2.5	◇		
MEA	×			1974.4	−1.0	1.1	×		
MGD	×			1978.0	−0.9	0.3	1975.0	−0.7	0.6
MIR	×			×			◇		
MIZ	*			◇			1975.0	−1.4	4.6
MLT	◇			×			*		
MMB	*			×			×		
MMK	×			1980.3	−1.3	1.0	1978.0	−3.9	2.1
MNK	×			1975.2	−0.9	1.1	1976.4	−2.1	1.8
MOL	×			×			×		
MOS	*			1978.0	−1.8	1.5	1977.9	−3.4	0.6
MUT	*			1978.6	−2.2	1.7	1979.0	−3.2	2.6
NAL	×			1978.2	−2.2	1.6	1974.0	−0.9	3.3
NCK	*			1978.4	−1.7	0.7	×		
NEW	×			×			*		
NGK	×			1978.2	−0.3	0.3	×		
NUR	×			1977.9	−0.7	0.7	1974.2	−1.1	1.7
NVL	1979.4	−5.0	1.5	×			◇		
NVS	×			1979.5	−3.6	1.6	1976.5	−1.8	1.3
ODE	×			1978.2	−0.8	0.7	×		
OTT	*			1979.8	−0.9	0.4	1976.3	−0.4	0.4
PAF	◇			1976.0	−1.1	0.9	1977.9	−3.5	0.6
PAG	×			1979.5	−0.8	1.4	◇		
PIL	×			1979.0	−0.7	0.4	◇		
PMG	1982.0	−4.6	0.5	1978.3	−0.8	0.8	1976.0	−.8	2.4
PPT	*			×			1977.4	−0.5	0.5
RES	×			1979.0	−0.7	0.6	◇		
SAB	×			1980.8	−2.0	1.1	1975.8	−1.6	0.6
SBA	◇			◇			1975.0	−1.6	4.2
SJG	*			1979.5	−1.4	1.0	1981.2	−4.2	1.1
SOD	×			1978.0	−0.5	0.4	1974.6	−1.1	1.5
SSH	×			1978.0	−2.2	1.6	1978.8	−3.5	1.6
STJ	◇			1976.0	−0.9	2.0	1978.7	−1.6	1.1
SUA	×			1981.4	−3.1	1.0	1978.0	−3.6	1.9
TAM	◇			×			◇		
TEN	◇			1978.0	−0.8	1.5	1975.3	−0.7	4.7

Table A2. (continued)

	X			Y			Z		
Observatory	τ	e_-	e_+	τ	e_-	e_+	τ	e_-	e_+
TEO	×			×			◇		
TFS	*			1978.2	−0.7	2.0	×		
THL	*			1980.3	−0.4	1.0	1980.0	−1.6	1.6
THY	1977.0	−1.7	4.2	1977.8	−0.5	0.5	×		
TIK	×			1978.0	−3.0	1.1	*		
TKT	*			◇			1975.7	−0.5	0.9
TNG	◇			1979.0	−1.0	3.7	×		
TRD	*			1978.0	−2.6	2.8	1979.0	−1.0	1.0
TRO	◇			1978.0	−0.7	0.9	×		
TRW	◇			◇			◇		
TSU	×			1981.8	−0.5	0.6	1981.0	−1.9	1.8
TTB	*			*			×		
VAL	×			1977.9	−0.2	0.3	1979.6	−2.9	1.2
VIC	*			1977.7	−0.3	0.5	1982.0	−1.3	0.7
VLA	×			1980.0	−5.3	0.9	1977.0	−2.4	3.5
VOS	×			◇			*		
VSS	◇			1978.6	−3.1	1.0	◇		
WHN	*			1975.2	−0.7	0.8	◇		
WIK	×			1978.2	−0.4	0.5	×		
WIT	×			1978.3	−0.3	0.3	×		
WNG	×			1978.0	−0.2	0.3	×		
YAK	×			1975.0	−1.0	0.5	1976.0	−1.2	1.1
YSS	×			×			×		

[a]See Table A1 footnote.

Table A3. Occurrence Date (τ) of the 1991 Geomagnetic Jerk[a]

	X			Y			Z		
Observatory	τ	e_-	e_+	τ	e_-	e_+	τ	e_-	e_+
AAA	1992.0	−0.1	0.2	◇			1990.1	−0.2	0.4
ABG	1992.2	−0.2	0.5	1995.0	−0.9	0.2	1990.8	−0.1	0.1
AIA	◇			1991.7	−1.3	0.9	◇		
ALE	*			*			◇		
AMS	1988.7	−0.3	0.3	1988.5	−0.7	0.7	1994.9	−0.3	0.2
API	◇			◇			1989.0	−0.2	0.2
AQU	◇			1990.1	−0.5	0.9	◇		
ARC	◇			◇			1990.5	−1.0	0.6
ARS	×			×			1992.4	−0.5	0.6
ASH	1995.0	0.0	0.1	1989.3	−1.0	0.4	1988.7	−0.7	0.8
BDV	◇			1990.0	−0.7	0.9	×		
BEL	◇			1990.4	−0.8	0.9	×		
BFE	◇			1990.8	−0.7	0.9	◇		
BJI	◇			1991.4	−0.5	0.5	1993.5	−0.3	0.3
BJN	1988.0	−1.1	0.2	1991.0	−1.0	1.7	×		
BLC	1992.1	−0.4	0.5	◇			◇		
BNG	◇			◇			1991.0	−0.4	0.1
BOU	1988.9	−0.5	0.2	1993.0	−0.4	0.6	1991.0	−0.4	0.4
BOX	×			1990.0	−1.7	0.6	1993.0	−0.6	0.6
BRW	1991.0	−0.7	0.9	1992.0	−2.3	2.7	◇		
CBB	◇			×			◇		
CCS	1993.0	−0.4	0.9	1990.0	−0.3	0.7	◇		
CDP	1995.6	−0.3	0.2	1991.3	−0.4	0.3	1988.0	−1.1	0.7
CLF	◇			1992.0	−0.9	0.5	◇		
CNB	1988.0	−0.3	0.6	◇			1988.3	−0.5	0.8
COI	1989.0	−0.3	0.2	1990.0	−0.1	0.2	◇		
CSY	×			◇			◇		

Table A3. (continued)

	X			*Y*			*Z*		
Observatory	τ	e_-	e_+	τ	e_-	e_+	τ	e_-	e_+
CTA	◇			×			◇		
CTS	1990.9	−1.3	0.2	×			◇		
CWE	◇			◇			1990.0	−0.2	0.1
CZT	1988.0	−0.2	0.4	1994.0	−2.8	1.0	1995.3	−0.5	0.3
DIK	◇			◇			1992.2	−0.3	0.2
DLR	1988.0	−0.1	0.8	1993.2	−0.8	1.8	1991.6	−0.3	0.3
DOB	1988.0	−1.5	1.0	1991.0	−0.7	0.7	◇		
DOU	◇			1991.2	−0.6	0.8	◇		
DRV	◇			1991.6	−0.9	1.1	1987.0	−0.6	4.0
DVS	×			1988.0	−0.1	0.6	◇		
ESK	1988.0	−0.4	0.9	1991.9	−0.9	0.6	◇		
ETT	1992.0	−2.8	2.9	1989.3	−0.9	1.2	1990.7	−0.1	0.1
EYR	◇			×			◇		
FCC	1992.0	−0.4	0.4	×			◇		
FRD	1988.4	−0.4	0.4	1992.5	−1.0	1.0	1991.2	−0.3	0.3
FRN	1988.0	−0.1	0.6	1994.4	−0.9	0.6	1989.0	−0.3	0.7
FUQ	◇			1992.0	−0.1	0.1	1992.1	−0.3	0.6
FUR	◇			1990.5	−0.7	0.9	◇		
GCK	◇			1990.0	−0.7	0.8	×		
GDH	1993.0	−0.3	0.7	1992.0	−1.1	4.0	1989.0	−0.6	1.9
GLN	1990.8	−1.1	0.5	◇			◇		
GNA	*						1991.4	−0.4	0.4
GUA	◇			×			1987.4	−0.5	0.6
GZH	◇			1992.2	−0.5	0.2	1991.0	−0.6	0.5
HAD	1988.0	−0.6	1.0	1991.9	−0.9	0.5	◇		
HBK	◇			1986.4	−0.4	0.5	◇		
HER	1989.0	−0.6	0.1	◇			◇		
HLP	◇			1990.9	−0.8	0.2	×		
HRB	◇			1990.8	−0.7	0.6	×		
HRN	◇			1990.1	−0.7	0.7	◇		
HTY	◇			◇			1994.1	−0.3	0.4
HYB	1992.0	−0.1	0.4	◇			1991.4	−0.1	0.1
IRK	1989.0	−0.5	1.8	1989.7	−0.3	0.8	◇		
ISK	◇			1990.1	−0.5	0.5	◇		
KAK	◇			◇			1994.0	−0.3	0.3
KIR	◇			1992.0	−0.7	0.9	1993.0	−0.4	0.5
KIV	◇			1990.0	−0.9	0.2	◇		
KNY	◇			1994.0	−2.4	1.4	1994.0	−0.2	0.4
KNZ	◇			◇			1994.0	−0.2	0.4
KOD	◇			1990.0	−0.2	0.2	◇		
KRC	×			×			◇		
LAS	◇			◇					
			◇						
LER	◇			1991.7	−1.1	0.8	◇		
LNN	◇			1990.0	−1.5	0.7	×		
LNP	◇			1992.0	−0.5	1.1	1992.0	−0.2	0.4
LOV	◇			1990.5	−0.6	1.0	◇		
LRV	1989.3	−0.8	1.3	1991.8	−1.1	0.9	1988.1	−0.2	0.8
LVV	◇			1987.7	−1.3	2.0	1993.0	−0.7	2.1
LZH	×			1990.6	−0.4	0.4	◇		
MAB	◇			1990.2	−0.5	1.6	◇		
MAW	×			◇			1993.0	−0.3	0.2
MBC	◇			◇			◇		
MBO	◇			◇			1986.4	−0.4	0.9
MCQ	1988.0	−0.7	0.8	1990.0	−0.9	3.5	1992.0	−0.5	0.7
MEA	1988.7	−0.4	0.4	1995.4	−0.6	0.4	◇		
MGD	◇			1994.0	−0.9	1.6	1991.0	−0.3	0.1
MIR	◇			◇			◇		
MIZ	◇			◇			1994.0	−0.3	0.3
MMB	1989.0	−0.9	0.5	◇			1993.7	−0.5	0.4
MNK	◇			1990.3	−0.5	1.3	×		

Table A3. (continued)

	X			Y			Z		
Observatory	τ	e_-	e_+	τ	e_-	e_+	τ	e_-	e_+
MOL	1989.9	−0.1	0.1	1990.0	−0.6	0.2	◇		
MOS	◇			1989.3	−0.4	0.7	1992.0	−0.4	0.2
MZL	◇			1991.4	−0.8	0.6	◇		
NAL	◇			◇			◇		
NAQ	1991.5	−0.7	1.1	×			1989.0	−0.7	0.1
NCK	◇			1991.0	−0.1	0.3	×		
NEW	1989.0	−0.6	0.3	1994.7	−0.9	0.9	1989.0	−0.8	0.5
NGK	◇			1990.5	−0.6	1.0	◇		
NUR	◇			1990.0	−0.5	1.0	×		
NVS	×			1994.0	−0.5	0.4	1991.0	−0.9	0.9
ODE	◇			1989.6	−1.7	0.5	×		
OTT	1988.8	−0.4	0.3	1993.0	−1.3	0.8	1992.6	−0.6	0.6
PAF	1988.2	−0.3	0.5	1988.0	−0.5	1.2	1993.7	−0.4	0.6
PAG	◇			1990.0	−1.0	0.9	×		
PBQ	1991.0	−0.2	0.3	1992.0	−0.7	0.2	◇		
PIL	◇			×			◇		
PPT	◇			1989.0	−0.4	0.9	×		
QGZ	1988.6	−0.3	0.4	1992.5	−0.3	0.3	1990.2	−0.7	1.0
QIX	◇			1991.6	−0.4	0.4	◇		
QUE	1992.0	−0.1	0.1	1993.0	0.0	0.1	◇		
QZH	◇			1993.9	−0.3	0.2	1991.9	−0.5	0.5
RES	1992.5	−0.9	1.1	◇			◇		
SAB	1993.3	−0.5	0.8	1988.0	−0.7	1.8	×		
SBA	×			1988.0	−1.9	0.5	1990.7	−0.9	1.3
SHL	◇			◇			◇		
SJG	1995.7	−0.3	0.2	1992.4	−0.9	0.7	1988.0	−0.4	0.4
SOD	◇			1990.3	−0.7	1.1	1993.3	−0.5	1.7
SPT	1988.0	−0.4	0.6	1991.6	−1.5	0.7	◇		
SSH	◇			1993.4	−0.7	0.5	1992.4	−0.3	0.3
STJ	1989.0	−0.4	0.4	◇			1989.7	−0.4	0.4
SUA	◇			◇			1995.6	−0.5	0.4
TEO	1991.0	−0.6	0.6	1994.4	−0.7	0.4	1994.0	0.0	0.1
TFS	1995.7	−0.3	0.3	1990.0	−0.4	0.7	1992.3	−0.6	0.5
THJ	◇			1990.6	−0.3	0.3	◇		
THL	1991.6	−1.1	1.3	×			◇		
THY	×			1991.0	−0.8	0.7	1995.0	−0.2	0.2
TKT	1995.0	−1.6	0.5	◇			1989.6	−0.9	1.4
TNB	1990.5	−1.2	0.1	◇			◇		
TNG	1989.6	−0.3	0.3	1995.0	−0.2	0.0	1991.0	−0.1	0.0
TRD	◇			1988.7	−0.3	0.3	1991.0	0.0	0.1
TRO	◇			1989.7	−0.7	0.9	×		
TRW	1988.0	−0.2	0.2	◇			1988.4	−0.5	0.7
TTB	◇			◇			◇		
UJJ	1993.0	−0.4	0.2	1994.4	−0.4	0.5	1989.0	−0.1	0.2
VAL	◇			1992.0	−0.8	1.1	1988.0	−0.5	0.7
VIC	1988.6	−0.4	0.5	1993.7	−0.9	1.1	◇		
VLA	×			◇			1992.4	−0.5	0.3
VSS	◇			1991.0	−0.3	0.2	◇		
WHN	◇			1992.5	−0.4	0.4	1994.4	−1.2	0.4
WIK	◇			1990.5	−0.9	0.8	×		
WMQ	1992.7	−0.4	0.4	1991.8	−0.5	0.5	*		
WNG	◇			1990.8	−0.7	0.9	◇		
YAK	◇			1991.8	−1.0	0.7	◇		
YKC	1989.5	−0.5	0.8	×			◇		

[a]See Table A1 footnote.

Table A4. Occurrence Date (τ) of the 1999 Geomagnetic Jerk[a]

	X			*Y*			*Z*		
Observatory	τ	e_-	e_+	τ	e_-	e_+	τ	e_-	e_+
ABG	◇			◇			◇		
ABK	◇			◇			◇		
AIA	2000.0	−2.0	0.4	◇			◇		
ALE	◇			◇			◇		
AMS	1999.3	−0.8	0.8	◇			◇		
API	◇			◇			1999.0	−0.4	1.2
AQU	◇			◇			◇		
ARS	◇			◇			◇		
ASH	◇			×			◇		
ASP	◇			×			◇		
BDV	◇			◇			◇		
BEL	1999.7	−1.9	0.5	◇			◇		
BFE	1998.0	−0.3	2.0	◇			◇		
BJN	◇			◇			◇		
BLC	◇			◇			◇		
BOU	◇			◇			◇		
BRW	◇			◇			◇		
BSL	◇			2000.0	−1.8	0.6	◇		
CBB	◇			◇			◇		
CBI	◇			×			◇		
CLF	1998.0	−0.3	1.6	×			2000.0	−1.3	0.7
CNB	◇			◇			◇		
COI	2000.0	−0.3	0.6	◇			2000.0	−0.9	0.3
CSY	◇			◇			◇		
CTA	◇			◇			◇		
CZT	◇			1998.9	−0.8	0.8	◇		
DLR	◇			◇			◇		
DOB	×			×			1999.6	−0.9	0.5
DOU	1998.2	−0.4	1.6	×			2000.0	−1.6	0.5
DRV	◇			◇			◇		
ESA	1998.0	−0.2	0.8	◇			◇		
ESK	1998.5	−0.6	1.5	×			2000.0	−0.5	0.7
EYR	◇			2000.0	−1.6	0.7	×		
FCC	◇			◇			1998.0	−0.6	0.5
FRD	◇			◇			◇		
FRN	◇			◇			◇		
FUR	◇			◇			◇		
GDH	◇			◇			◇		
GNA	◇			1999.0	−0.6	0.5	◇		
GUA	◇			2000.0	−2.0	0.4	1998.3	−0.3	0.2
GUI	◇			◇			◇		
HAD	1998.5	−0.6	1.4	×			×		
HBK	1998.0	−0.2	0.4	◇			◇		
HER	◇			◇			×		
HLP	1999.0	−1.2	1.1	◇			◇		
HRB	1999.0	−1.2	1.4	1999.0	−1.9	0.2	◇		
HRN	◇			◇			◇		
HTY	1998.3	−0.4	0.5	◇			◇		
IRK	◇			◇			◇		
KAK	2000.0	−0.2	0.3	◇			◇		
KIR	×			◇			2000.4	−0.4	0.3
KNY	◇			×			◇		
KNZ	◇			◇			◇		
LER	1998.0	−0.9	1.4	×			2000.0	−1.7	0.5
LOV	×			◇			◇		
LRM	◇			2000.4	−1.1	0.3	◇		
LRV	◇			1998.0	−0.6	1.3	2000.0	−0.6	0.6
LZH	◇			×			◇		
MAB	1998.0	−0.4	1.4	◇			1999.9	−1.4	0.7
MAW	◇			2000.6	−0.7	0.4	◇		
MCQ	◇			◇			1998.0	−0.6	0.6

Table A4. (continued)

	X			*Y*			*Z*		
Observatory	τ	e_-	e_+	τ	e_-	e_+	τ	e_-	e_+
MEA	◇			◇			1998.0	−0.8	0.7
MIR	◇			◇			◇		
MIZ	1998.0	−0.2	1.2	◇			◇		
MMB	1998.0	−0.4	0.2	◇			◇		
MOS	◇			◇			◇		
NAQ	◇			◇			◇		
NCK	◇			◇			◇		
NEW	◇			◇			◇		
NGK	◇			◇			◇		
NUR	1998.0	−1.0	0.5	◇			1998.1	−0.5	1.4
NVS	◇			◇			◇		
ODE	◇			◇			◇		
OTT	◇			◇			◇		
OUL	1998.6	−0.8	1.3	×			◇		
PAF	◇			◇			◇		
PAG	1998.0	−0.4	0.8	◇			1998.0	−0.8	0.9
PBQ	◇			◇			◇		
PPT	×			◇			×		
QUE	◇			×			◇		
RES	◇			◇			◇		
SBA	◇			◇			◇		
SJG	◇			◇			1999.0	−1.5	1.0
SOD	×			◇			1999.9	−0.6	0.6
SPT	◇			◇			◇		
STJ	◇			◇			◇		
SUA	◇			×			◇		
TAM	◇			◇			◇		
TAN	◇			◇			◇		
TFS	◇			◇			◇		
THL	◇			×			◇		
THY	◇			◇			◇		
TKT	*			*			◇		
TRO	◇			◇			◇		
TSU	1998.0	−0.6	0.1	◇			◇		
TTB	2000.0	−2.1	0.5	×			◇		
VAL	1998.4	−0.5	1.6	1998.0	−0.5	0.9	×		
VIC	◇			◇			1998.0	−0.6	1.5
VNA	◇			×			◇		
WNG	◇			◇			◇		
YKC	◇			◇			◇		

[a]See Table A1 footnote.

Table A5. Number of Observatories Included, Excluded, and Not Detected in the Data Analysis of Each Geomagnetic Jerk for the Annual Mean Data Sets[a]

	Annual Means														
	Included			Not Detected			Excluded			Error on Date			Error on Amplitude		
Jerk	*X*	*Y*	*Z*	*X*	*Y*	*Z*	*X*	*Y*	*Z*	*X*	*Y*	*Z*	*X*	*Y*	*Z*
1970	78	90	69	31	18	19	14	15	19	−1.5	−0.9	−1.5	−0.8	−0.4	−1.0
										1.9	1.0	1.3	0.8	0.4	0.9
1978	43	93	66	15	12	24	67	20	35	−1.7	−1.2	−1.8	−1.1	−0.5	−1.2
										1.7	1.1	1.6	1.3	0.4	1.1
1991	43	90	59	73	32	58	23	17	23	−1.5	−1.1	−1.2	−1.5	−0.4	−0.9
										1.9	1.1	1.4	0.9	0.4	0.9
1999	21	9	14	70	73	77	9	36	10	−1.0	−1.2	−1.3	−0.4	−0.6	−0.5
										1.4	0.8	1.0	0.4	0.6	0.6

[a]The mean error bars upper limit (first line for each jerk) and lower limit (second line) of the date occurrence (in years) and amplitude (in nT/yr^2) for each geomagnetic jerk are also given. The mean error bars on the 1969, 1978, and 1991 jerk occurrence times of the *X*, *Y*, and *Z* components are 1.7, 1.1, and 1.5 years, respectively.

Table A6. Summary of Nine Previous Works on the Detection of Geomagnetic Jerks, Specifying the Data, the Methods Used, and Which Jerks Were Detected

	Data	Method	Jerks
Le Mouël et al. [1982]	annual means (X, Y Z) 130 observatories	LS fit two straight-lines	1969
Le Huy et al. [1998]	smoothed annual means 160 observatories	LS fit two straight-lines	1969, 1978, 1991 global
Alexandrescu et al. [1996]	monthly means: comb. of X and Y 74 observatories	Wavelet analysis	1901, 1913, 1925, 1932, 1949, 1969, 1978
De Michelis et al. [2000]	annual means (X, Y and Z) 109 observatories	LS fit two straight-lines	1991 global
Mandea et al. [2000]	monthly means (Y) 12 month running average	Visual	1999 jerk in 9 observatories
Nagao et al. [2003]	monthly means (X, Y and Z) ≈ 50 observatories	Statistical model LS fit two straight-lines	1969, 1978, 1991 global
Chambodut and Mandea [2005]	monthly means (Y) and synthetic data from CM4	Wavelet analysis/LS fit two straight-lines	1969, 1978, 1991 global(?)
De Michelis and Tozzi [2005]	monthly means 44 observatories	Wavelet analysis Local Intermittency Measure	1978, 1991, 1999 global 1986 local
Olsen and Mandea [2007]	satellite monthly means (virtual observatories)	Spherical Harmonic Expansion/LS fit two straight-lines	2003
Present work	annual and monthly means and synthetic data from CM4	LS fit two straight-lines	1969, 1978, 1991 global 1999 not detected

Acknowledgments

[59] The results presented in this paper rely on data collected at magnetic observatories. We thank the National Institutes that support them and INTERMAGNET for promoting high standards of magnetic observatory practice (http://www.intermagnet.org). We thank S. Macmillan for the useful and motivating discussions and suggestions during the development of this work and also N. Olsen for helpful comments on jerk data analysis. Katia Pinheiro was partially supported by a Dorothy Hodgkin Postgraduate Studentship.

References

Alexandrescu, M., D. Gilbert, G. Hulot, J.-L. Le Mouël, and G. Saracco (1995), Detection of geomagnetic jerks using wavelet analysis, *J. Geophys. Res.*, *100*, 12,557–12,572.

Alexandrescu, M., D. Gilbert, G. Hulot, J.-L. Le Mouël, and G. Saracco (1996), Worldwide wavelet analysis of geomagnetic jerks, *J. Geophys. Res.*, *101*(B10), 21,975–21,994.

Alldredge, L. R. (1977), Deep mantle conductivity, *J. Geophys. Res.*, *82*(33), 5427–5431.

Alldredge, L. R. (1984), A discussion of impulses and jerks in the geomagnetic field, *J. Geophys. Res.*, *89*, 4403–4412.

Chambodut, A., and M. Mandea (2005), Evidence for geomagnetic jerks in comprehensive models, *Earth Planets Space*, *57*, 139–149.

Chulliat, A., and K. Telali (2007), World monthly means database project, *Publ. Inst. Geophys. Polish Acad. Sci.*, *C99*(398), Inst. of Geophys., Polish Acad. of Sci., Warsaw.

Chulliat, A., E. Thébault, and G. Hulot (2010), Core field acceleration pulse as a common cause of the 2003 and 2007 geomagnetic jerks, *Geophys. Res. Lett.*, *37*, L07301, doi:10.1029/2009GL042019.

Courtillot, V., and J.-L. Le Mouël (1984), Geomagnetic secular variation impulses, *Nature*, *311*, 709–716.

De Michelis, P., and R. Tozzi (2005), A local intermittency measure (LIM) approach to the detection of geomagnetic jerks, *Earth Planet. Sci. Lett.*, *235*, 261–272.

De Michelis, P., L. Cafarella, and A. Meloni (2000), A global analysis of the 1991 geomagnetic jerk, *Geophys. J. Int.*, *143*, 545–556.

Gubbins, D. (2004), *Time Series Analysis and Inverse Theory for Geophysicists*, Cambridge Univ. Press, Cambridge, U. K.

Gubbins, D., and J. Bloxham (1985), Geomagnetic field analysis—III. Magnetic fields on the core-mantle boundary, *Geophys. J. R. Astron. Soc.*, *80*, 695–713.

Gubbins, D., and L. Tomlinson (1986), Secular variation from monthly means from Apia and Amberley magnetic observatories, *Geophys. J. R. Astron. Soc.*, *86*, 603–616.

Haines, G. V. (1993), Modelling geomagnetic secular variation by main-field differences, *Geophys. J. Int.*, *114*, 490–500.

Le Huy, M., M. Alexandrescu, G. Hulot, and J.-L. Le Mouël (1998), On the characteristics of successive geomagnetic jerks, *Earth Planets Space*, *50*, 723–732.

Le Mouël, J.-L., J. Ducruix, and C. H. Duyen (1982), The worldwide character of the 1969–1970 impulse of the secular acceleration rate, *Phys. Earth Planet. Inter.*, *28*, 337–350.

Lowes, F. J. (1966), Mean-square values on sphere of spherical harmonic vector fields, *J. Geophys. Res.*, *71*, 2179.

Malin, S. R. C., and B. M. Hodder (1982), Was the 1970 geomagnetic jerk of internal or external origin?, *Nature*, *296*, 726–728.

Mandea, M., and N. Olsen (2009), Geomagnetic and archeomagnetic jerks: Where do we stand?, *Eos Trans. AGU*, *90*(24), 208.

Mandea, M., E. Bellanger, and J.-L. Le Mouël (2000), A geomagnetic jerk for the end of the 20th century?, *Earth Planet. Sci. Lett.*, *183*, 369–373.

Mandea Alexandrescu, M., D. Gilbert, J.-L. Le Mouël, G. Hulot, and G. Saracco (1999), An estimate of average lower mantle conductivity by wavelet analysis of geomagnetic jerks, *J. Geophys. Res.*, *104*(B8), 17,735–17,745.

Menke, W. (1989), *Geophysical Data Analysis: Discrete Inverse Theory*, *Int. Geophys. Ser.*, vol. 45, Academic, San Diego, Calif.

Nagao, H., T. Iyemori, T. Higuchi, S. Nakano, and T. Araki (2002), Local time features of geomagnetic jerks, *Earth Planets Space*, *54*, 119–131.

Nagao, H., T. Iyemori, T. Higuchi, and T. Araki (2003), Lower mantle conductivity anomalies estimated from geomagnetic jerks, *J. Geophys. Res.*, *108*(B5), 2254, doi:10.1029/2002JB001786.

Olsen, N., and M. Mandea (2007), Investigation of a secular variation impulse using satellite data: The 2003 geomagnetic jerk, *Earth Planets Space*, *255*, 94–105.

Olsen, N., and M. Mandea (2008), Rapidly changing flows in the Earth's core, *Nat. Geo.*, *1*, 390–394.

Parker, R. (1994), *Geophysical Inverse Theory*, Princeton Univ. Press, Princeton, N. J.

Pinheiro, K., and A. Jackson (2008), Can a 1D mantle electrical conductivity model generate magnetic jerk differential time delays?, *Geophys. J. Int.*, *173*(3), 781–792.

Sabaka, T. J., N. Olsen, and R. A. Langel (2002), A comprehensive model of the quiet-time, near-earth magnetic field: phase 3, *Geophys. J. Int.*, *151*, 32–68.

Sabaka, T. J., N. Olsen, and M. E. Purucker (2004), Extending comprehensive models of the Earth's magnetic field with Ørsted and CHAMP data, *Geophys. J. Int.*, *159*, 521–547.

Sivia, D. S., and J. Skilling (2006), *Data Analysis, A Bayesian Tutorial*, 2nd ed., Oxford Univ. Press, Oxford, U. K.

Walker, M., and A. Jackson (2000), Robust modelling of the Earth's magnetic field, *Geophys. J. Int.*, *143*(3), 799–808.

Whaler, K. A. (1987), A new method for analysing geomagnetic impulses, *Phys. Earth Planet. Inter.*, *48*, 221–240.